Precambrian Research, 50 (1991) 111–136
Elsevier Science Publishers B.V., Amsterdam

Short-lived Eburnian orogeny in southern Mali. Geology, tectonics, U–Pb and Rb–Sr geochronology

J.P. Liégeois[a], W. Claessens[a,1], D. Camara[b] and J. Klerkx[a]
[a]*Department of Geology, Musée Royal de l'Afrique Centrale, B-2080 Tervuren, Belgium*
[b]*Direction Nationale de la Géologie et des Mines, Bamako, Mali*

(Received November 27, 1989; accepted after revision August 15, 1990)

ABSTRACT

Liégeois, J.P., Claessens, W., Camara, D. and Klerkx, J., 1991. Short-lived Eburnian orogeny in southern Mali. Geology, tectonics, U–Pb and Rb–Sr geochronology. Precambrian Res., 50: 111–136.

This work is based on a comprehensive field survey, including mapping of the Massigui degree sheet in southern Mali. The investigated area belongs to the northern part of the Man shield which is mainly composed of Lower Proterozoic volcano-sedimentary sequences (Birimian) and of large areas of granitoids, the whole being affected by the Eburnian orogeny.

Structural and geochronological (U–Pb and Rb–Sr) results from this study point to a short period of time (~30 Ma) for the Eburnian orogenesis between 2100 and 2070 Ma, the events recorded later (1984 ± 30 Ma) being due to tectonic reactivations. On the other hand, no trace of events older than 2100 Ma have been found. Coupled with geochemical and Rb–Sr isotopic systematics, this leads to invoke a fundamental link between Birimian volcanics and Eburnian granitoids, both being high-K calc-alkaline in composition and coming from a single, evolving mantle source in a palaeo-environment which has some of the characteristics of modern subduction (including back-arc) or docking zones.

The main regional structure of the area strikes roughly NNE–SSW with an important strike-slip component, escorted by a greenschist metamorphism. The deformation is the most intense in the N40° to N10° 5 km large Banifin shear-zone where metamorphism reached the lower amphibolite facies. Here one observes subvertical strong foliation, non-cylindrical folding (locally sheath folds) and subhorizontal pencil lineations, the deformation being regionally recorded by light sub-isoclinal folds with subvertical axes compatible with a sinistral movement.This regional shear tectonics (D_2,2074+9/−8 Ma) is preceded by an isoclinal deformation (D_1, bracketed between 2098 ± 5 Ma and D_2) only known as relics, from which it likely derived. A later phase (D_3) occurred along the Banifin shear belt, at a more superficial level, even if still ductile, generated by a dextral movement and having induced retrograde metamorphism. This last tectonic phase, which is not accompanied by plutonism nor volcanism, has been dated at 1982 ± 30 Ma, being responsible for the complete resetting of the Rb–Sr isotopic system in the plutons present in the Banifin corridor.

Introduction

The West African craton has been stable since the end of Early Proterozoic, not much after 2 Ga. It is surrounded by Pan-African belts [Trans-Saharian, Mauritanides (reactivated during Variscan orogeny), Rockellides, Fig. 1], its southern boundary being in fact in South America (Lesquer et al., 1984; Hurley et al., 1967). Its central part is covered by a huge cratonic basin (Taoudenni) whose sediments display ages from 1 Ga to Carboniferous, for the essential.

Two shields crop out to the north and to the south of this basin, Reguibat and Man, respectively, with two small inliers in a central west position, Kayes and Kenieba. The western parts of the shields are composed of Archaean

[1]Present address: Department of Geology and Mining, Klöckner Industrie Anlangen GmbH, D-4100 Duisburg, FRG.

0301-9268/91/$03.50

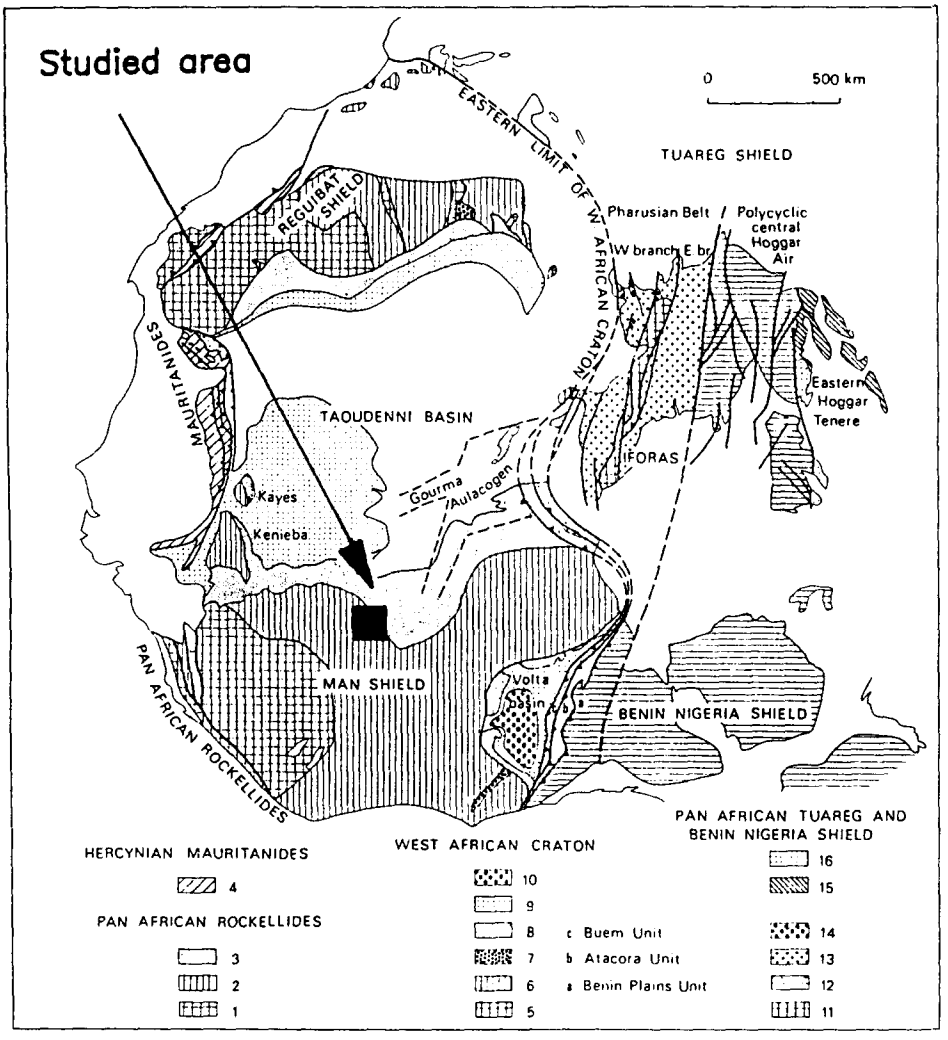

Fig. 1. Schematic map of major Precambrian units of the West African craton overthrusted on its edges by the Pan-African belts (Black, 1980). *1*=Archaean (?) of the Kasila Group. *2*=Lower Proterozoic, Marampa Group. *3*=Upper Proterozoic, Rockell Group. *4*=Metamorphosed undifferentiated Precambrian and Lower Palaeozoic. *5*=Archaean. *6*=Lower Proterozoic (including the Birimian). *7*=Middle (?) Proterozoic including the Tarkwaian and Guelb el Hadid Groups. *8*=Upper Proterozoic of the Taoudenni basin and the Togo belt. *9*=Late Precambrian and Cambrian (?) of the Taoudenni and Volta basins. *10*=Upper Voltaian. *11*=Archaean. *12*=Polycyclic basement of the Tuareg shield. *13*=Upper Proterozoic (Pharusian). *14*=Ahnet Purple series. *15*=Undifferentiated Upper (?) Proterozoic. *16*=Tiririne Group.

rocks practically unaffected by later events, whereas to the east the essential imprints are of Lower Proterozoic age. In Man, the boundary between these two domains is not definitely known, but is traditionally associated with the Sassandra-Mt Trou faults.

The Lower Proterozoic domain (Fig. 2) is often referred to as Baoule–Mossi domain in the Man shield (Fig. 1). Classically, it is composed of volcano-sedimentary sequences, called Birimian, and of large areas of granitoids, the whole being affected by the Eburnian orogeny. More recently, Lemoine et al. (1986) have suggested the existence of two successive cycles, the Burkinian deformation affecting the Dabakalian series followed by deposition of the Birimian, the whole being folded by the Eburnian episode. Unfortu-

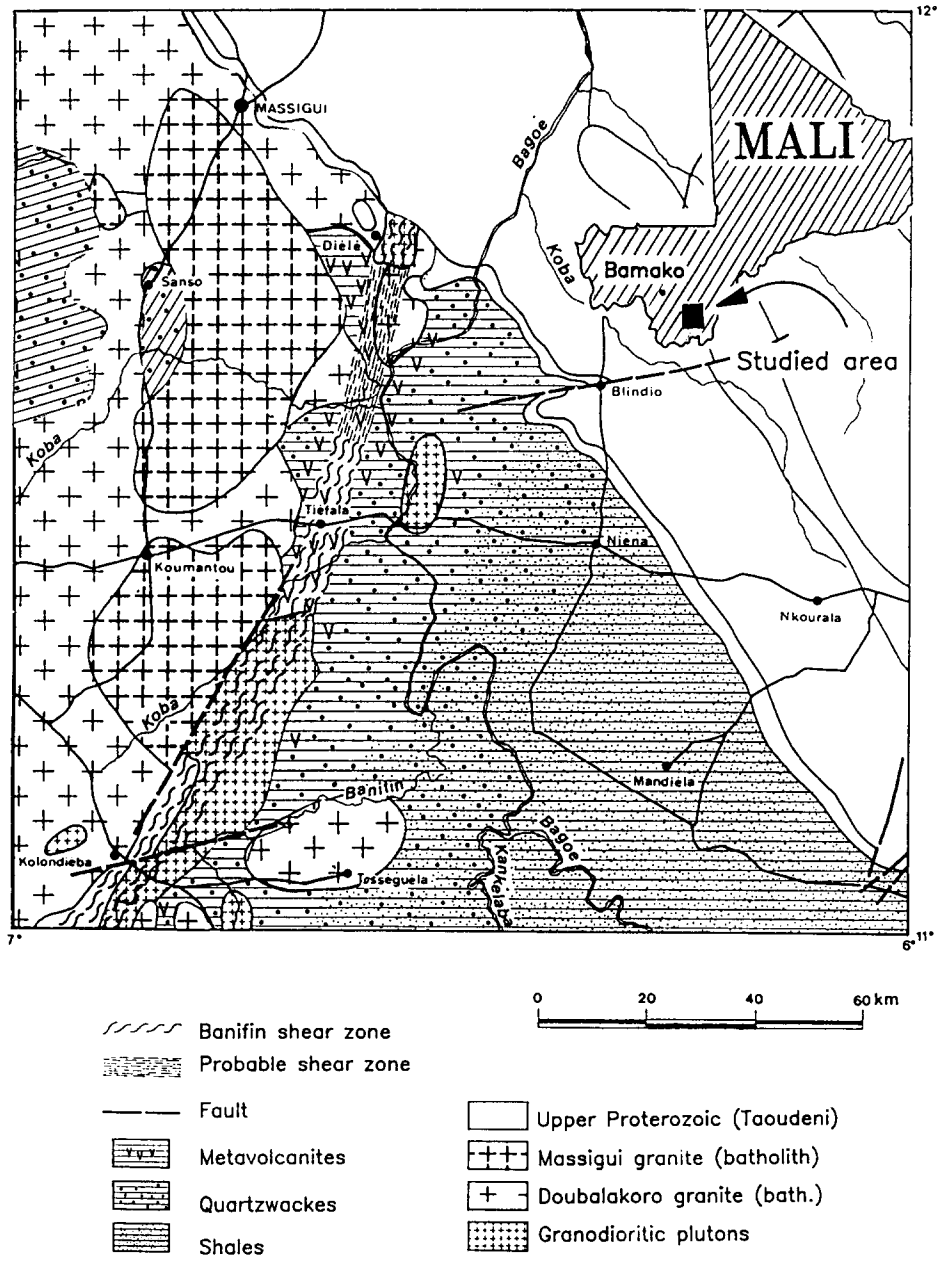

Fig. 2. Geological map of the studied area, located in Mali (inset). The quartzwackes in the northwestern part of the area (around Sanso and to the west) belong to the Kekoro–Bougouni unit while the major part of the metasediments (west of the batholith) belongs to the Bagoe unit.

nately this is based on geochronological data not yet published. In fact, the classical long-lasting Eburnian period (2400–1600 Ma, Bessoles, 1977) cannot correspond to one orogenesis and one must define the real duration of the Eburnian.

The axes of this study were, on the basis of precise field data, to decipher the succession of events which occurred in southern Mali, to settle them in time with accurate radiochronol-

ogical data, to know the relationships between plutonic and volcanic rocks and finally to rough out a geodynamical palaeo-environment.

Lithologies

The studied area is situated to the north of the Man shield in southern Mali between 5° and 7°E and 11° and 12°N. Except the northeastern part which belongs to the Taoudenni basin, it is located in the Lower Proterozoic domain. The latter comprises essentially a volcano-sedimentary domain which is intruded by several intrusions, with a huge granitic batholith.

The volcano-sedimentary group

Two volcano-sedimentary series are present in the Massigui degree sheet, separated by an important intrusive unit (Fig. 2):
- a small area in the northwest composed of quartzites which belong to the Kekoro–Bougouni unit (Spindler, 1952);
- a series present in all the southeastern part of the studied area and which constitutes the northern part of the Bagoe unit (Bassot et al., 1981). It is composed of acid to intermediate volcanic rocks with rare basalts and of metasedimentary rocks (quartzwackes and shales). No unconformity on an older basement has been found.

The Bagoe series is a NNE–SSW supracrustal belt which extends in Ivory Coast for several hundreds of kilometres and which disappears to the north under the Taoudenni basin. It comprises three lithological units: the eastern part is composed of shales, the western part by metavolcanics and the centre by quartzwackes (Fig. 2). The boundaries are progressive even the western limit of the quartzwackes where intercalations of lavas appear progressively, becoming more and more abundant to the west.

The shales: a pelitic formation with gold-bearing dykes

The eastern part of our area crops out very badly. Only outcrops of shales have been found but intercalations of quartzwackes and small bodies of intrusive rocks probably exist as shown by their presence as float.

These shales have been metamorphosed in the greenschist facies and are essentially composed of two rock types. The first is a gray sericito-schist with a well-developed cleavage while the second is ferruginous and more compact.

Characteristic for this formation is the presence of siliceous rocks. Generally they appear as dykes associated in stockwork, but in the south (Tingrela area) exist subvertical jasper bands, discontinuous and metric to decametric in width. Gold anomalies are spatially related to these siliceous formations, dykes or jaspers. Some of these jaspers are associated with basalts and pillow lavas (Diallo and Kusnir, 1985); a part of the shale formation could then be of volcano-sedimentary origin (tuffs).

To the east, this sequence grades to a heterogeneous formation composed of polygenic conglomerates, quartzites and volcanic breccias. It is not clear if this formation belongs to the Birimian (Bassot et al., 1981) or is younger, i.e., Tarkwaian (Diallo and Kusnir, 1985), as no contact has been seen.

The quartzwackes: an immature series

To the west, the volcano-sedimentary series become progressively less pelitic and more siliceous. Some volcanic intercalations, essentially porphyritic basalts, become more abundant westward. Petrographically, the dominant facies is composed of impure sandstones or quartzwackes following the classification of Dott (1964). Composed of 30 to 60% of a matrix composed of micas and quartz, they comprise fragments essentially of quartz (around 90%) but also lithic (10%) and very minor detrital feldspars. Some rocks in minor amount could be qualified as graywackes.

Within this lithology crops out also conglomerates and quartz-bearing shales. This series shows sedimentary structures, the stratification being generally subvertical. Younging deductions are not easy but it seems that the bottom of the basin is to the east, the volcanics being then younger, which is in agreement with data from eastern Senegal (Ledru et al., 1989). We must not forget however that the apparition of volcanics is progressive and consequently that there is no major break between sediments and volcanics.

The volcanics: an intermediate series

As for the transition shales–quartzwackes, the transition quartzwackes–volcanics is progressive. The volcanics predominate in the Diele–Tiefala–Kolondieba axis (Fig. 2). They have variable compositions but intermediate compositions prevail, essentially rhyodacites and andesites, even if rhyolites and basalts are also present. To the north, volcanic breccias and agglomerates are abundant. The mineralogy of these volcanics is characteristic of the greenschist facies.

The intrusive complex

Two groups of intrusives have been distinguished. The first one is essentially of intermediate composition and situated in or near the Banifin corridor while the second is of granitic composition and extends just west of the Banifin tectonic area (Fig. 2).

The intrusive nature of the granitoids is attested by the presence among the enclaves of volcanic and volcano-sedimentary material typical of the Birimian volcano-sedimentary group.

The plutons of intermediate composition

This unit comprises two important plutons (Sodioula and Diele) trending N–S in the Banifin corridor and two smaller plutons, Koue and Pankourou respectively cropping out east and west of Banifin (Fig. 2).

Their compositions vary from quartz-diorite through quartz-monzodiorite to granodiorite; granite compositions are very scarce. Petrographically, undeformed Sodioula-type rocks show a granoblastic assemblage of plagioclase, microcline, quartz, hornblende and biotite. Partially amphibolitized clinopyroxene is sometimes present. The rocks of this group have generally a fine and equigranular texture, except Diele which often presents a coarse-grained and porphyritic texture. Diele is also conspicuous for the numerous pegmatitic and aplitic dykes which cut it essentially following a NNE–SSW trend.

The granitic batholiths

The granite compositions grade from biotite-rich monzogranite to potassic leucogranite. These rocks show a foliation only locally and often near contacts. The latter are irregular and frequently constituted of migmatites and agmatites, both grading to quartzo-feldspathic dyke networks intruded into the volcano-sedimentary units following the schistosity planes.

The predominant enclaves are of basic composition. They are mainly concentrated in some areas of the pluton where it can appear as a hybrid body. There, the foliation is often well-marked and the enclaves are much elongated and look like schlieren. This suggests that these areas could be the border of pulses where the combination of tectonics and magmatic convection has allowed the rise of more mafic rocks, which could be the magmatic precursors of the granitoids. This implies that these granitoids are subcontemporaneous to the deformation.

The small number of outcrops has only allowed a rough mapping of the granitoids. Two main rock types have been recognized: (1) a rather homogeneous potassic pink leucogranite (Massigui type); (2) a group of various biotite granites (Doubalakoro type).

The principal varieties of the Doubalakoro type vary from a fine- to medium-grained bio-

tite-rich granite which approaches a granodiorite to a biotite-poor and K-feldspar-rich granite which approaches the Massigui-type granite. The Massigui granite has been distinguished because of its greater homogeneity and because it extends over a large area (half of the granite surface, in two plutons; Fig. 2). As Doubalakoro pendants are present in the Massigui pluton, the latter postdates the former.

Granodiorites, quartz-diorites and diorites are associated with the granites. They appear most frequently as enclaves but they can sometimes form small plutons. However, the association of this large variety of rock types from diorites to potassic leucogranites through granodiorites, monzogranites and syenogranites indicates a fairly complete magmatic suite.

Metamorphism

Except in the Banifin shear belt, the metamorphic parageneses observed in the sedimentary and in the volcanic sequences are homogeneous: quartz–biotite–albite–(epidote–chlorite) in the quartzwackes, quartz–albite–biotite–epidote–(actinolite–chlorite) in the acid volcanics and actinote–epidote–albite–biotite–(quartz–chlorite) in the basic volcanics. They are characteristic of the transition between the chlorite and the biotite zone of the greenschist facies. These metamorphic minerals are fine-grained and granoblastic. No porphyroblasts have been observed. The phyllosilicates and the amphiboles are oriented and mark the schistosity which indicates the syntectonic character of this regional metamorphism.

In the Banifin band, along the granitic batholith, the metamorphism, as well as the deformation, is more intense, the mineral assemblages being characteristic of the lower amphibolite facies. It is not clear if this higher metamorphism is connected to the proximity of the batholith as in eastern Senegal (Ndiaye et al., 1989) or to the greater intensity of the deformation, both causes being probably linked. Some of the samples show a retrograde metamorphism in the greenschist facies (recristallisation of amphibole and biotite as epidote, sphene and chlorite) associated with cataclasis at the border of phenocrysts, phenomena linked to the polyphase character of the Banifin band and the circulation of fluids (see below).

Tectonics

Regional structure

The general NNE–SSW trend of the Bagoe unit corresponds to the general orientation of Birimian basins ("sillons") of the Baoule–Mossi domain. However, in the north of the studied area, the volcano-sedimentary sequences, as well as the Massigui pluton, swing progressively to the N and NNW. To the west, the Kekoro–Bougouni unit has a similar shape.

The volcano-sedimentary sequences show a subvertical schistosity oriented N0° to N40°, parallel to the regional structure, well-developed in the pelitic rocks and moderately to weakly developed in the arenaceous or volcanic lithologies. This schistosity is sometimes parallel to the sedimentary bedding but more often it is slightly oblique to it, the intersection lineation being subvertical or at least with a steep plunge, indicating decametric to hectometric tight folds with steep axis. This regional schistosity cuts in some places an older foliation always parallel to the bedding which can be related to a first isoclinal tectonic phase. The poor number of good outcrops do not allow a detailed study of the structure and to know if there has been tectonic thickening during this first event. This phase can perhaps be correlated to the regional phase described by Ndiaye et al. (1989), which has the same characteristics.

Narrow subvertical shear-zones have been observed in the pelitic facies where they display subhorizontal movements along a well-developed schistosity as shown by the sub-hor-

izontal stretching lineation and the local occurrence of assymetric folds with subvertical axes. The adjacent and less affected quartz-wacke layers are often characterized by extensional cracks sometimes sigmoidal and generally filled by quartz. Sinistral sense of movements is deduced from the fold patterns, whereas dextral sense is indicated by the tension gashes. It will be shown hereafter that these two senses of movement are related to two successive events (D_2 and D_3) separated by 100 Ma. The similarity between the assymetric folds structure in the discrete shear-zones and the tight sub-isoclinal folding on a regional scale leads to invoke a single tectonic event. This second tectonic phase is then related to a regional sinistral strike-slip regional mechanism whilst the first regional tectonics is poorly known, its main characteristic being that the schistosity is always parallel to the bedding.

The Banifin shear belt

The Banifin shear belt is a NNE–SSW subvertical shear-zone 5 km large. It was identified for the first time by an aeromagnetic survey (Barinkov and Novikov, 1966) and studied later during strategic prospecting by the BRGM and the DNGM (Buchstein et al., 1974). In Mali, it extends over 100 km from the Ivory Coast border to the Taoudenni basin where it disappears beneath the Upper Proterozoic cover (Fig. 2). To the south, the Banifin shear zone possibly joins the Sassandra-Mt Trou major shear zone (Fig. 1).

In the studied area, the Banifin shear zone stretches roughly between the Massigui–Doubalakoro granitic batholith and the Bagoé unit which is in this area essentially of volcanic composition (Fig. 2). The elongated plutons of intermediate composition, Sodioula and Diélé occur in this zone of intense deformation and often display, particularly the former, well-oriented rock fabrics.

In the volcano-sedimentary sequence, the foliation, always in subvertical position, is locally folded in decimetric to decametric folds, with steep axis (60° to 80°) and non-cylindrical character which is also characteristic of the Comoé Series in eastern Ivory Coast (Vidal, 1987). The schistosity plane is frequently marked by a stretching lineation roughly perpendicular to the fold axis and showing subhorizontal (Tefiala area) or oblique (30° to 40° SSE, Kolondieba area) directions. Some of the fold structures give evidence for sinistral subhorizontal to oblique slip. In strongly foliated zones, subhorizontal sheath folds have been observed. The schistosity is essentially marked by biotite and amphibole which swing around feldspathic and lithic clasts.

A later phase is materialized by extensional cracks mostly filled by quartz appearing locally in the more competent lithologies. Their orientations, in opposition to the fold structures, suggest dextral movement of the shear. In the area between Tiéfala and Kolondiéba, occur subvertical pegmatitic veins, showing the same directions as the above mentioned cracks. Their emplacement can be linked to the retrograde metamorphism and cataclasis occurring in the Banifin corridor and imply then the polyphase character of the latter. This last event has been called D_3 deformation.

In the plutons of intermediate composition, the Banifin deformation event is characterized by a variable intensity, stronger in Sodioula than in Diélé. Sodioula is generally marked by a penetrative subhorizontal pencil lineation oriented N0° to N25°, whereas Diélé records discrete subvertical bands where the shear is intense and comparable to Sodioula between zones only slightly affected. In the eastern part of the Diélé pluton, the numerous pegmatitic dykes are oriented N20°E which probably correspond to zones of weakness created by the late reactivation of the shear. On the whole in Sodioula and in the deformed parts of Diélé, the rock textures are clearly mylonitic but show that the strain intensity has varied considerably laterally. This mylonitisation consists of partially granulated and twisted feldspars and

of recrystallised quartz ("mortar structure") in elongated zones underlined by biotite and sericite schlieren which deviate around porphyroclastic augen. Less affected rocks show sometimes that the mylonitisation is superimposed on an original granoblastic oriented texture. This superposition can be seen, but rarely well, on some outcrops.

In summary, both plutonites and volcanites in the Banifin shear belt display two deformation events: (1) The first one occurred in ductile conditions and is assumed to fit in a NNE–SSW shear regime of sinitral sense; it has evolved in amphibolite facies metamorphic conditions. The oriented magmatic texture and the elongated shapes of the granodiocitic intrusives suggest a syn- to late-tectonic emplacement relatively to this phase. (2) A second phase, which, when present, most often obliterates the first one, but which can be sometimes seen as superimposed, is also characterized by a shear regime and affects particularly the Sodioula pluton. A greenschist retrograde metamorphism is contemporaneous. Subhorizontal movements along subvertical planes are likely and extensional cracks indicate a dextral slip during this second event.

During the first shearing phase, the Banifin corridor acted in fact as a zone of maximum intensity of shear, roughly situated at the contact between the granitic batholith and the volcano-sedimentary sequences. We are dealing with an important shear zone, with strong foliation, local intense folding and the occurrence of sheath folds whose intensity decreases rapidly to the east creating tight subisoclinal folding with subvertical axis on a regional scale (Fig. 3). This last fact requires that the volcano-sedimentary beds were sufficiently inclined before folding and is incompatible with a simple basin configuration. This can perhaps be linked to the existence of the older isoclinal phase which could be an early stage of the same phase. More work, probably in other regions where this D_1 phase will better appear, is necessary to assess t his point. To the west, the huge

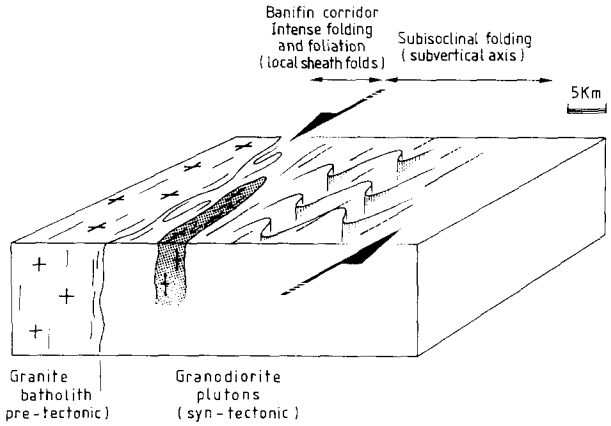

Fig. 3. Schematic three-dimensional representation of the D_2 deformation characteristics in the studied area. From west to east: minor shear bands in the batholith; intense deformation along the batholith (Banifin shear zone, sinistral movement) in the Birimian and the granodioritic plutons marked by intense schistosity, pencil lineation and sheath folds; in the major part of the Birimian, subisoclinal folds with subvertical axis.

granitic batholith is only locally affected by the D_2 deformation and has generally an equant texture, the batholith having reacted as a rigid core.

Deformation in granites

Structurally, the Massigui granite has been classified as post-tectonic (Bassot et al., 1981), on the basis that generally it shows an isotropic fabric. However, we consider the batholith, including Doubalakoro, as pre- to early-tectonic following the observation that it shows zones with more or less intense foliation as it is also the case in eastern Senegal (Ledru et al., 1989). Indeed, this heterogeneous deformation in granitoid bodies is characteristic of tectonics with an important shear component. Saharian areas, where outcrops are quasi-continuous, show in a beautiful manner this heterogeneous response of magmatic bodies submitted to shear movements (Liégeois et al., 1987). Moreover, in Burkina Faso, 200 km east of our area, Legrand (1971) has demonstrated with U–Pb on zircon datations that plutons originally considered as post-tectonic based on the

same lack of uniform deformation, were in fact clearly pre-tectonic (2135 Ma) relatively to the main regional deformation (2065 Ma). The tectonic characterization of granitoids is often delicate (Paterson and Tobisch, 1988), but here the evidence indicates that the batholith is pre-to early-tectonic with respect to D_2 and may be to D_1 is D_1 and D_2 are two stages of the same deformation.

Conclusions

A first isoclinal regional deformation, probably tangential (S_0 parallel to S_1) has affected the volcano-sedimentary sequences but is poorly known. For reasons of convenience, we shall call it D_1 without necessarily separating it from the next one. The main structure of the area is due to the second regional phase (D_2) which is characterized by an important sinistral shear component inducing tight folds with subvertical axis and which was accompanied by a regional greenschist facies. The maximum strain intensity (intense foliation and non-cylindrical folding) is reached in the Banifin band, at the contact between the granitic batholith and the volcano-sedimentary sequences, where syn- to late-tectonic granodioritic plutons intruded (Fig. 3) and metamorphic grade attained the amphibolite facies. Similar characteristics have been found in Ivory Coast for the main deformation in the Comoé unit (Vidal, 1987; Vidal and Alric, 1987). Subsequently and apparently restricted to the Banifin corridor occurred an intense reactivation (D_3) of the shear at a higher structural level in low greenschist facies conditions.

Geochronology

Analytical techniques

The measurements have been done on a Finnigan MAT 260 thermal ionisation mass spectrometer.

Rb–Sr: After acid dissolution of the sample and Sr separation on ion-exchange resin, Sr isotopic composition is measured on Re double filament. The $^{87}Sr/^{86}Sr$ of NBS987 standard (normalized to $^{88}Sr/^{86}Sr=0.1198$) during the course of this study was 0.710221 ± 0.000019. The ages have been calculated following Williamson (1968) and all the errors are given at the 2σ level. Used ^{87}Rb disintegration constant is 1.42×10^{-11} a^{-1} (Steiger and Jäger, 1977). Rb and Sr concentrations have been measured

TABLE 1

U–Pb on zircon data.

Sample fraction	U (ppm)	Pb* (ppm)	$^{206}Pb/^{204}Pb$	$^{206}Pb^*/^{238}U$	$^{207}Pb^*/^{235}U$	$^{207}Pb^*/^{206}Pb^*$
CW714a (Tin Fouga rhyo-dacite)						
3°M/ 63–106 μm	622	167	1298± 6	0.2260	3.9157	0.12563
1°M/100–150 μm	446	122	2193±44	0.2338	4.1296	0.12809
−1°M/ 63–100 μm	382	131	3218±85	0.2951	5.2306	0.12854
−3°M/ 63–250 μm	311	119	3716±27	0.3307	5.8883	0.12912
CW711a (Sodioula granodiorite)						
−1°M/ 63–100 μm	446	144	1454±11	0.2964	5.2049	0.12734
−3°M/100–150 μm	472	157	1946± 5	0.3074	5.4155	0.12776
−5°M/ 63–100 μm	325	119	2224±12	0.3350	5.9043	0.12781

M = magnetic; the negative sign (−) signifies that the zircon fraction is diamagnetic. The sign (*) indicates radiogenic part of the considered isotope. Errors on U and Pb concentrations and then on $^{207}Pb^*/^{235}U$ and on $^{206}Pb^*/^{238}U$ ratios are less than 1%. Error on $^{207}Pb/^{206}Pb$ ratio, depending on the knowledge of isotope fractionation, is less than 0.1%; between-run errors are typically ten times better.

by X-ray fluorescence. The error on the Rb/Sr ratio is less than 2% when concentration of both elements are above 30 ppm.

U–Pb: The method is derived from that of Krogh (1973) modified by Lancelot (1975). Zircon is classically separated by shake table, heavy liquids, Frantz isodynamic magnetic separator, following their size and finally by hand-picking under binocular. After dissolution of 2 to 5 mg pure and homogeneous zircon fraction, aliquots are taken for composition and concentration, the latter being mixed with ^{204}Pb enriched spike. Pb and U are separated on ion exchange resin (Dowex 100–200) micro-columns, being eluated respectively in HCl and H_2O medium. Pb and U are measured on Re single filament with the silica-gel technique between 1100° and 1200°C where the fractionation coefficient is known at better than 0.1% and is equal to 0.09% per a.m.u. The following disintegration constants were used (Steiger and Jäger, 1977): $^{235}U = 9.8485 \times 10^{-10}\,a^{-1}$; $^{238}U = 1.55125 \times 10^{-10}\,a^{-1}$. The intercepts with Concordia and errors have been calculated following Ludwig (1980).

Results

Two U–Pb on zircon discordia (7 fractions, Table 1) and five Rb–Sr isochrons (41 whole rocks, Table 2) have been obtained.

Outside of the Banifin corridor, the volcanics have given with the U–Pb method an upper intercept of 2098 ± 5 Ma and a lower intercept of 135 ± 18 Ma (four zircon fractions, MSWD = 0.01, Fig. 4a) and with the Rb–Sr method an age of 2073 ± 38 Ma ($^{87}Sr/^{86}Sr$ initial ratio (SrIR) = 0.70181 ± 0.00010, 7WR, MSWD = 2.50, Fig. 4b). The granitic batholith (Massigui–Doubalakoro) has given a Rb–Sr age of 2091 ± 33 Ma (SrIR = 0.7021 ± 0.0003, 15WR, MSWD = 1.33, Fig. 4c). A small granitic pluton (Sirakoro) located east of the Banifin corridor (Fig. 2) has given a younger age of 1974 ± 76 Ma (SrIR = 0.7019 ± 0.0016, 4WR, MSWD = 0.84, Fig. 4d). Let us remark

TABLE 2

Rb–Sr on whole rock data.

Sample	Rb (ppm)	Sr (ppm)	$^{87}Rb/^{86}Sr$	$^{87}SR/^{86}Sr \pm 2\sigma$
Tin Fouge volcanites				
CW714A	216	252	2.497	0.77884 ± 0.00004
CW97	144	108	3.899	0.81800 ± 0.00009
CW151C	75.3	868	0.251	0.70942 ± 0.00004
CW169D	179	343	1.515	0.74527 ± 0.00007
CW227D	79.8	682	0.339	0.71223 ± 0.00003
CW325B	11.7*	709	0.0478	0.70322 ± 0.00003
CW333A	182	823	0.6406	0.72027 ± 0.00005
Doubalakoro-Massigui batholith				
CW721A	146	557	0.760	0.72529 ± 0.00004
CW721B	95.0	706	0.389	0.71377 ± 0.00003
CW721C	123	698	0.510	0.71784 ± 0.00003
CW721D	105	863	0.352	0.71286 ± 0.00004
CW721F	152	292	1.512	0.74780 ± 0.00005
CW721G	171	245	2.030	0.76134 ± 0.00005
CW721I	308	208	4.336	0.83145 ± 0.00004
CW722A	528	33.2	53.053	2.27154 ± 0.00006
CW715B	112	598	0.542	0.71785 ± 0.00001
CW715C	91.9	704	0.378	0.71348 ± 0.00002
CW715E	127	232	1.590	0.74917 ± 0.00005
CW715F	89.9	543	0.479	0.71657 ± 0.00003
CW720A	98.6	46.2	6.291	0.89922 ± 0.00006
CW720B	92.2	52.5	5.158	0.86269 ± 0.00005
CW720C	96.4	42.0	6.768	0.90391 ± 0.00007
Sirakoro granitic pluton				
CW724A	185	414	1.297	0.73945 ± 0.00009
CW724B	178	417	1.239	0.73745 ± 0.00002
CW724C	157	162	2.824	0.78228 ± 0.00004
CW724D	147	55.6	7.810	0.92261 ± 0.00008
CW724F	156	391	1.157	0.73382 ± 0.00003
CW724G	157	421	1.082	0.73270 ± 0.00001
Sodioula granodioritic pluton				
CW711A	150	489	0.889	0.72734 ± 0.00008
CW712A	159	447	1.032	0.73179 ± 0.00008
CW712B	141	517	0.790	0.72535 ± 0.00006
CW712C	143	426	0.973	0.73069 ± 0.00005
CW713A	212	205	3.016	0.78939 ± 0.00006
CW713B	243	185	3.838	0.80999 ± 0.00003
CW713C	253	197	3.753	0.80997 ± 0.00007
Diele granodioritic pluton				
CW716A	129	498	0.751	0.72428 ± 0.00003
CW716C	65.6	946	0.2006	0.70812 ± 0.00004
CW717A	147	197	2.171	0.76398 ± 0.00003
CW717B	142	212	1.947	0.75774 ± 0.00006
CW717C	172	121	4.158	0.82018 ± 0.00003
CW718D	76.9	780	0.2853	0.71070 ± 0.00003
CW718E	77.8	740	0.417	0.71477 ± 0.00003
CW719A	339	716	1.375	0.74219 ± 0.00005
CW819B	142	404	1.019	0.73183 ± 0.00007

Sr en Rb concentrations by XRF except (*) by isotope dilution.

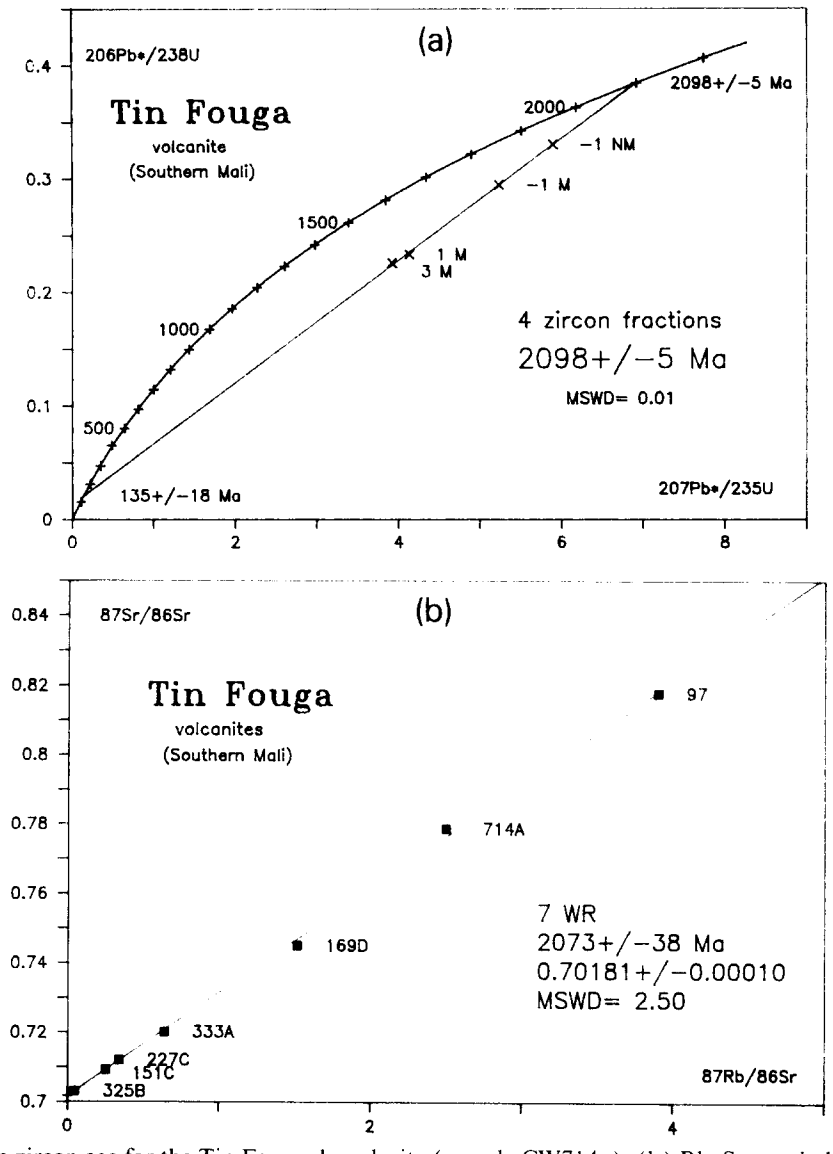

Fig. 4. (a) U–Pb on zircon age for the Tin Fouga rhyo-dacite (sample CW714a). (b) Rb–Sr on whole rock isochron of the Tin Fouga volcanite. (c) Rb–Sr on whole rock isochron of the Massigui-Doubalakoro granitic batholith. (d) Rb–Sr on whole rock isochron of the small granitic pluton of Sirakoro. (e) U–Pb on zircon age of the Sodioula syn-tectonic granodioritic pluton (sample CW711a). (f) Rb–Sr on whole rock isochron of the Sodioula granodioritic pluton. (g) Rb–Sr on whole rock isochron of the Diele granodioritic pluton.

here already that all the samples of this isochron come from a single complex outcrop of only several square metres.

Inside the Banifin corridor, the Sodioula granodioritic pluton has given with the U–Pb method an upper intercept of $2074+9/-8$ Ma and a lower intercept of 81 ± 75 Ma (3 zircon fractions, MSWD=0.35, Fig. 4e) while the Rb–Sr method has given a younger age of 1975 ± 61 Ma (SrIR=0.7026 ± 0.0011, 7WR, MSWD=0.64, Fig. 4f). The other granodioritic pluton, Diélé, has given with the Rb–Sr method an age of 1992 ± 39 Ma (SrIR=0.70248 ± 0.00026, 9WR, MSWD=0.63, Fig.

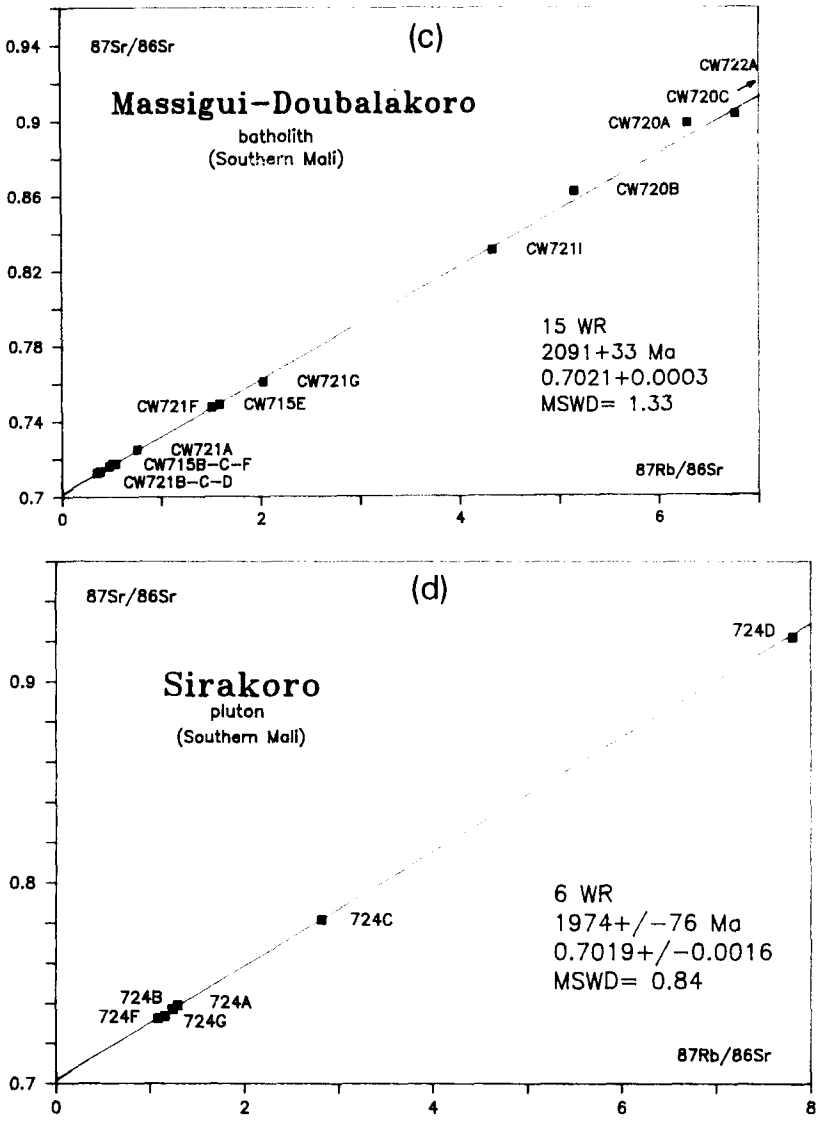

Fig. 4. Continued.

4g). All the results are reported in Fig. 5.

The lower intercepts of the zircon discordia are probably geologically meaningless and may correspond to a continuous lead loss although a thermal perturbation linked to Atlantic opening cannot be definitely ruled out. More or less recent Pb loss due to incipient weathering is also possible (Black, 1987). The degree of discordance of the zircon fractions are remarkably correlated to their magnetism, their U and Pb content and anti-correlated to their $^{206}Pb/^{204}Pb$ ratio (Table 1).

Interpretation

The different ages of this study have been reported in Fig. 5. The two U–Pb on zircon ages are interpreted as emplacement ages. The Sodioula granodiorite being syn-D_2, the zircon age ($2074+9/-8$ Ma) corresponds to both the time of deformation and intrusion. The zircon age of the Tin Fouga volcanics (2098 ± 5 Ma) being distinct, even within error limits, from this age, it does not correspond to the deformation but to the extrusion of the volcan-

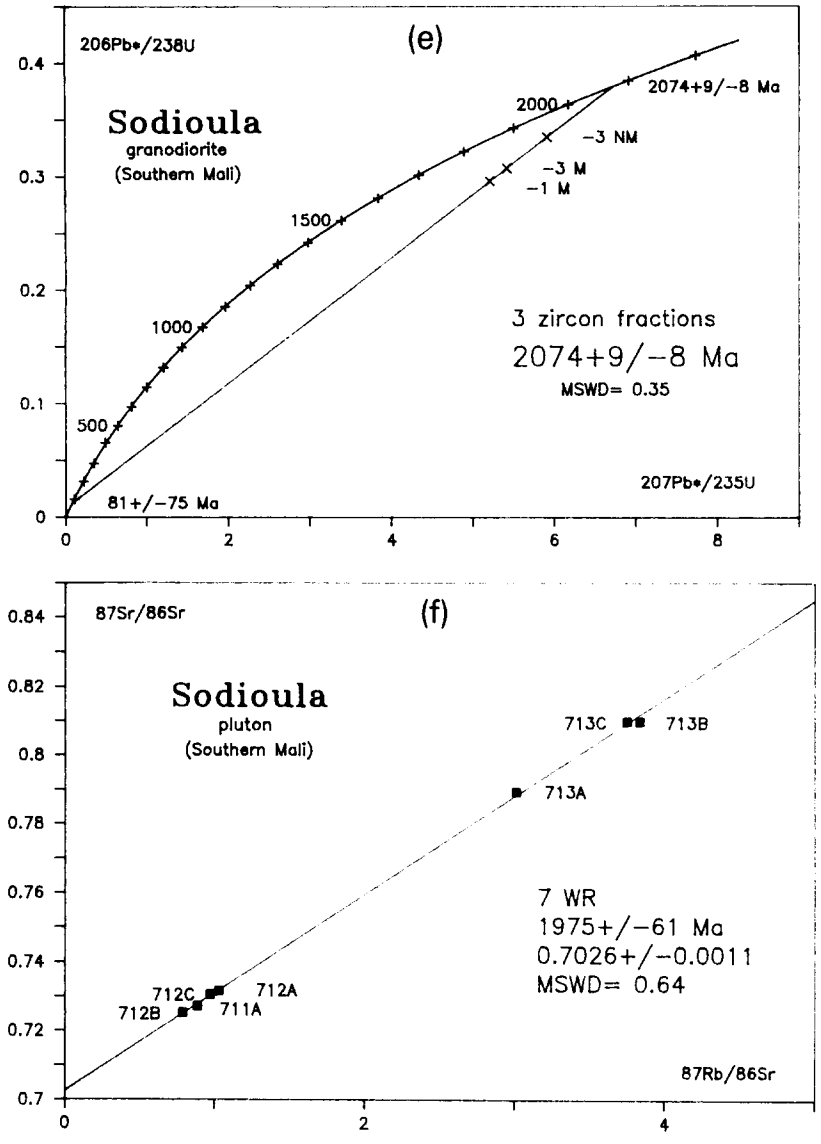

Fig. 4. Continued.

ics. The collected sample is only weakly affected by tectonics which confirms this interpretation. As these volcanics are pre-D_1, these two zircon ages imply that D_1 tectonics occurred between 2098 ± 5 Ma and 2074 + 9/ − 8 Ma. The same age bracket can be applied to the Massigui–Doubalakoro batholith as it is intrusive in the volcanics and is anterior to the granodiorites. Its Rb–Sr data (2091 ± 33 Ma) is in agreement with this time interval but could also correspond, within error limits, to the deformation. In the same way, the Rb–Sr age of the volcanics (2073 ± 38 Ma) encompasses the age of the emplacement and of the deformation.

These two Rb–Sr ages are distinct from the Rb–Sr results of the three other plutons, Sodioula (1975 ± 61 Ma), Diélé (1992 ± 39 Ma) and Sirakoro (1974 ± 76 Ma), as shown in Fig. 5. This clearly distinct set of ages can only

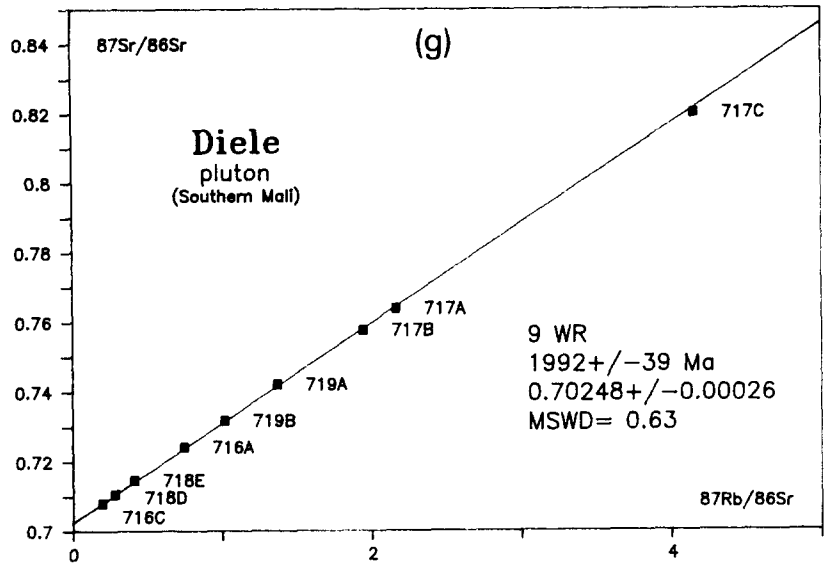

Fig. 4. Continued.

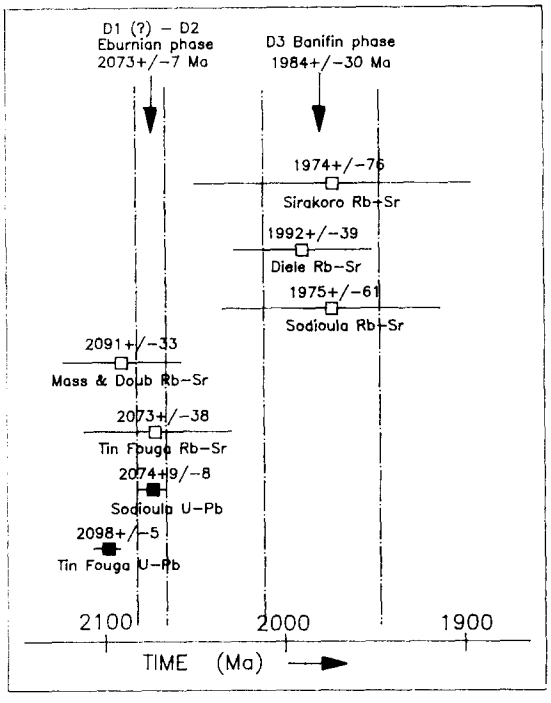

Fig. 5. Summary of the different ages obtained in this study showing the extrusion age of the Birimian volcanics is just older than the main Eburnian deformation followed about 100 Ma later by the D_3 tectonic reactivation, restricted to the Banifin shear zone.

comply with an isotopic rehomogeneisation, as we know with the U–Pb data on zircon, that the Sodioula granodiorite emplacement age is significantly older ($2074+9/-8$ Ma). This later perturbation can easily be attributed to the D_3 deformation which has strongly affected Sodioula and Diélé plutons and not the granitic batholith nor the analyzed volcanics. The good quality of the isochrons can likely be credited to percolation of fluids associated with the retrograde greenschist metamorphism present in the Banifin shear belt. Although the Sirakoro pluton lies just outside the Banifin corridor, its age can be attributed to the same phenomenon as all the samples come from a single, small, complex outcrop, a disposition which favours the recording of a rehomogeneisation age.

A mean age, weighted by the errors, of the D_3 deformation can be calculated with these three Rb–Sr ages; it gives 1984 ± 30 Ma, an age which can be considered as that of the D_3 deformation in the Massigui area.

The geochronological data (Fig. 5) lead to four important conclusions:

(1) the entire magmatism occurred during a relatively short period of time, between 2098

Ma and 2073 Ma, except perhaps some pegmatites if their link with D_3 can be proven. This implies a fundamental link between the "Birimian" volcanism and the "Eburnian" plutonism.

(2) D_1 cannot be much older than D_2 (between 0 Ma and 25 Ma) which is in favour of the interpretation of one deformation which evolves from a tangential regime to a shear regime. By opposition, the D_3 deformation is a much later reactivation (around 100 Ma later) of some D_2 structures whose origin can be absolutely distinct from the D_1–D_2 Eburnian deformation.

(3) Although field observations are not unambiguous, they support the idea that the volcanic rocks are at the top of the Birimian sequence. However, as the transition from the sediments to the volcanics is progressive and the sediments are immature, representative of a relatively rapid sedimentation, the sediments of the area cannot be much older than the volcanics. In fact, we would easily accept the suggestion of Barning (1987) and Milesi et al. (1987) that the sediments and the volcanics are sub-contemporaneous. There is then no evidence in the area for the existence of the so-called Dabakalian unit and Burkinian orogeny of Lemoine et al. (1986).

(4) The good quality of the isochrons corresponding to the D_3 deformation indicates that Sr isotopic rehomogeneisation can occur at a kilometric scale in greenschist facies, then in wet conditions, during shear tectonics when circulation of fluids is important. This last condition is essential as volume diffusion alone is an effective mechanism only over distances of a few centimetres when Rb–Sr isochrons resulting from a regional rehomogeneisation actually exist (Cliff, 1985).

The regional or local character of this chronological model needs to be assessed with combined U–Pb on zircon and Rb–Sr on whole-rocks or on mineral datations elsewhere, but some previous data and current studies seem to indicate that it could be regional, the different geological events being, of course, not rigorously synchronous:

- Legrand (1971) has shown that some granites from Burkina Faso considered as post-tectonic are in fact pre- or syn-tectonic, the main Eburnian deformation being dated around 2100 Ma (Ledent et al., 1969; Legrand, 1971).
- Bassot and Caen-Vachette (1984) have already noted the possibility of tectono-metamorphic resetting of the Rb–Sr system because of the existence of discrepancies between geochronological and field data: similar plutons give ages of 2045 ± 27 Ma (Gamaye) and 1973 ± 33 Ma (Saraya).
- The minimum age for the intrusion of Cape Coast granite pluton in Ghana is 2051 ± 45 Ma (Agyei et al., 1987).
- In the Sassandra area, in Ivory Coast, Feybesse et al. (1989) arrive to the same timing as the present authors for the Eburnian orogeny; precise comparison is not possible as geochronological data are not yet published.
- Current studies in South Mali give Rb–Sr ages around 1950 Ma (UNDP project and Liégeois, in prep.) and in West Mali Rb–Sr ages around 1950 Ma and U–Pb on zircon ages around 2080 Ma (Klöckner project and Liégeois, in prep.).

If it is confirmed that the resetting of the Rb–Sr isotopic system occurring around 1950–1980 Ma in some plutons is a regional phenomenon, this implies that carefulness in the interpretation of ages is necessary when only Rb–Sr data are available (e.g. Bassot and Caen-Vachette, 1984) particularly if they show complex patterns (Toure et al., 1987) and in geological deductions as, for example, the major break in sediment deposition between 2150 Ma and 1970 Ma proposed by Bertrand et al. (1989).

Geochemistry and strontium initial ratios

The samples have been analyzed (Table 3) for the major elements (XRF and AA) and for four trace elements (Rb, Sr, Y, Zr) by XRF in

TABLE 3

Major and trace elements.

	SiO_2	TiO_2	Al_2O_3	Fe_2O_3	FeO	MnO	MgO	CaO	K_2O	Na_2O	P_2O_5	P.F.	Total	Zr	Y	Sr	Rb
Sodioula																	
CW771A	65.57	0.47	15.19	1.44	2.41	0.06	2.37	3.58	3.87	3.87	0.20	1.13	100.16	191	16	489	150
CW711B	65.77	0.45	15.09	1.50	2.39	0.06	2.48	3.48	3.94	3.77	0.15	1.07	100.15	187	15	472	152
CW711C	66.32	0.47	14.97	1.67	2.20	0.06	2.25	3.45	3.74	3.76	0.16	1.08	100.13	135	4	551	179
CW712A	70.65	0.19	14.81	1.10	0.70	0.02	0.64	1.45	6.19	3.59	0.12	0.72	100.18	225	11	447	159
CW712B	64.26	0.54	15.25	1.58	3.08	0.07	3.06	4.05	3.50	3.95	0.18	1.18	100.70	203	17	517	141
CW712C	66.86	0.38	14.82	1.32	2.22	0.07	2.25	3.24	4.06	3.86	0.14	1.07	100.29	160	15	426	143
CW712D	67.95	0.24	14.82	1.07	1.39	0.05	1.81	2.60	5.28	3.59	0.10	0.83	99.73	140	14	419	148
CW712E	66.09	0.47	14.83	1.50	2.58	0.08	2.70	3.42	3.55	4.19	0.13	1.18	100.72	177	15	425	152
CW712F	62.92	0.55	15.19	1.86	2.99	0.07	3.36	4.14	3.57	3.98	0.26	1.18	100.07	208	16	553	150
CW713A	72.59	0.20	13.77	0.60	0.91	0.03	0.37	1.19	5.25	3.71	0.19	0.67	99.48	157	11	205	212
CW713B	73.10	0.19	13.97	0.51	0.91	0.03	0.30	1.21	5.21	3.78	0.10	0.54	99.85	155	13	185	243
CW713C	72.23	0.22	13.91	0.57	1.04	0.04	0.37	1.07	5.62	3.65	0.12	0.67	99.51	173	12	197	252
CW221B	65.70	0.47	14.40	1.05	2.73	0.05	2.26	3.27	4.22	3.46	0.15	1.09	98.88				
CW345B	65.11	0.51	14.46	1.49	2.79	0.06	2.78	3.68	3.50	4.10	0.15	1.10	99.73				
CW350C	74.13	0.13	13.09	0.32	0.77	0.03	0.24	0.84	5.38	3.79	0.07	0.58	99.37				
Diele																	
CW716A	64.37	0.54	15.71	1.38	2.94	0.08	1.60	3.27	3.97	4.35	0.22	1.16	99.59	229	23	498	129
CW716B	58.32	1.33	16.68	2.64	4.91	0.11	1.67	4.76	2.33	4.58	0.37	1.60	99.30	190	18	798	73
CW716C	56.46	1.59	16.78	2.98	5.30	0.15	2.27	5.54	1.96	4.78	0.51	1.41	99.73	176	23	946	66
CW716D	64.68	0.56	15.66	1.86	2.61	0.07	1.54	3.33	3.67	4.45	0.23	1.14	99.80	252	22	521	124
CW716E	64.57	0.55	15.95	1.52	2.77	0.01	1.84	3.28	3.81	4.51	0.22	1.14	100.17	228	21	523	142
CW717A	70.74	0.25	14.30	0.69	1.20	0.04	0.64	1.13	5.15	4.25	0.17	0.89	99.45	185	17	197	147
CW717B	71.44	0.25	14.40	0.98	0.93	0.04	0.46	1.19	5.08	4.28	0.17	0.84	100.06	198	15	212	142
CW717C	73.90	0.07	13.65	0.44	0.39	0.02	0.17	0.76	4.96	4.48	0.11	0.73	99.68	69	12	121	172
CW718A	55.65	1.04	16.72	3.08	4.58	0.11	3.77	6.35	2.75	4.06	0.51	1.67	100.29	232	22	833	93
CW718B	55.01	1.40	16.56	4.38	4.21	0.13	2.84	6.08	2.39	4.60	0.68	1.52	99.80	212	24	873	78
CW718C	56.99	0.91	16.68	2.42	5.70	0.13	3.19	6.71	2.05	3.76	0.26	1.51	100.31	152	26	644	68
CW718D	56.11	0.81	16.95	3.22	4.24	0.11	3.46	6.12	2.54	3.83	0.26	1.96	99.61	195	20	780	77
CW718E	56.53	1.15	15.67	2.78	7.12	0.14	3.21	6.27	2.17	3.44	0.33	1.60	100.41	214	26	540	78
CW719A	60.81	0.70	17.33	2.60	3.31	0.10	2.24	4.14	2.12	4.63	0.29	1.34	99.61	244	20	716	339
CW719B	68.05	0.41	14.91	1.39	1.87	0.06	1.11	2.47	4.31	4.00	0.19	0.89	99.66	188	19	404	142
CW87A	64.74	0.54	14.82	1.82	2.68	0.07	1.65	3.29	3.73	4.10	0.23	1.18	98.85				
Doubalakoro																	
CW721A	67.79	0.43	14.64	1.12	1.84	0.05	1.56	2.47	4.19	4.15	0.19	0.89	99.32	193	13	557	146
CW721B	56.35	0.67	15.40	2.48	5.01	0.12	4.32	6.86	2.12	4.61	0.29	1.20	99.43	175	20	706	95
CW721C	61.82	0.77	17.34	2.02	3.49	0.07	1.87	4.04	1.92	5.36	0.29	1.16	100.15	244	14	698	123
CW721D	59.12	0.62	18.32	1.81	3.14	0.07	2.74	5.11	1.91	5.13	0.24	1.31	99.52	245	18	863	105
CW721E	69.76	0.34	14.51	0.83	1.07	0.05	0.52	1.32	5.02	4.35	0.05	0.82	98.63	229	18	257	162
CW721F	68.19	0.33	15.33	1.35	1.98	0.06	1.34	2.00	4.13	4.23	0.10	1.02	100.06	226	17	292	152
CW721G	70.28	0.32	14.33	1.13	0.77	0.04	0.51	1.18	4.95	4.34	0.10	0.83	98.78	223	19	245	171
CW721H	71.81	0.24	13.76	0.57	0.92	0.02	0.49	1.24	5.53	3.57	0.08	0.93	99.16	174	14	208	307
CW721I	71.97	0.25	14.12	0.57	0.99	0.02	0.46	1.19	5.51	3.45	0.10	0.93	99.56	198	15	203	305
CW722A	76.69	0.09	12.76	0.43	0.38	0.05	0.20	0.47	4.56	3.86	0.05	0.76	100.30	61	30	33	528
CW 41C	70.95	0.22	15.46	0.53	0.89	0.03	0.72	1.75	3.08	5.70	0.11	0.72	100.16				
CW203A	67.59	0.42	14.38	1.68	1.78	0.06	1.34	2.80	4.13	4.31	0.16	0.81	99.46				

TABLE 3 (continued)

	SiO_2	TiO_2	Al_2O_3	Fe_2O_3	FeO	MnO	MgO	CaO	K_2O	Na_2O	P_2O_5	P.F.	Total	Zr	Y	Sr	Rb
Massigui																	
CW715A	51.74	0.65	14.63	2.89	6.11	0.17	7.50	7.77	2.26	3.82	0.24	1.66	99.44	148	19	540	76
CW715B	52.75	0.81	14.68	2.07	6.10	0.13	7.61	6.80	3.05	2.28	0.40	2.00	99.68	223	21	598	112
CW715C	51.78	0.82	15.18	2.12	6.32	0.14	8.26	7.43	2.73	3.14	0.43	1.90	100.25	191	19	704	92
CW715D	58.99	0.57	14.75	2.90	4.12	0.14	4.61	5.66	1.70	4.61	0.21	1.35	99.61	192	25	427	85
CW715E	69.71	0.30	15.18	1.77	0.88	0.05	0.60	1.56	5.12	4.83	0.09	0.74	100.83	245	25	232	127
CW715F	62.93	0.60	15.95	2.26	3.13	0.07	1.43	4.15	2.82	4.15	0.24	1.14	99.87	256	25	543	90
CW720A	73.07	0.17	14.34	0.91	0.79	0.04	0.09	0.79	5.92	4.03	0.03	0.40	100.58	223	13	46	99
CW720B	71.61	0.21	14.54	0.90	0.84	0.04	0.10	0.84	5.88	4.26	0.05	0.47	99.74	290	13	53	92
CW720C	72.30	0.18	14.25	0.75	0.80	0.04	0.08	0.76	6.03	4.09	0.05	0.40	99.73	231	11	42	96
CW 19A	70.66	0.34	13.28	1.32	1.40	0.05	0.51	1.30	4.97	4.14	0.12	0.70	98.79				
CW107A	74.23	0.11	12.60	0.59	0.39	0.02	0.10	0.70	4.69	4.64	0.04	0.49	98.60				
CW124A	69.18	0.26	14.75	1.35	1.15	0.04	0.50	1.77	5.76	3.90	0.12	0.69	99.47				
CW124B	65.82	0.53	15.74	1.91	2.09	0.06	1.02	3.13	3.07	4.58	0.24	1.10	99.29				
CW124C	55.06	0.83	17.29	2.58	5.23	0.11	2.92	6.55	1.86	4.40	0.24	1.55	98.62				
CW156C	74.31	0.10	13.19	0.40	0.46	0.02	0.11	0.68	5.93	3.31	0.03	0.72	99.26				
CW343A	68.08	0.24	16.20	1.20	0.73	0.05	0.36	0.92	6.24	5.10	0.05	0.97	100.14				
CW366A	77.07	0.06	12.08	0.45	0.29	0.01	0.06	0.41	5.21	3.81	0.02	0.33	99.80				
Sirakoro																	
CW724A	70.80	0.22	14.72	0.90	0.76	0.02	0.49	1.58	4.97	4.20	0.15	1.04	99.85	187	10	414	186
CW724B	70.42	0.22	14.73	0.01	1.52	0.02	0.51	1.49	4.81	4.16	0.10	0.92	98.91	205	9	417	178
CW724C	77.12	0.14	12.47	0.58	0.16	0.01	0.13	0.38	6.50	2.93	0.03	0.47	100.92	100	7	162	157
CW724D	76.39	0.14	12.08	0.65	0.11	0.01	0.10	0.32	6.36	3.38	0.03	0.35	99.92	106	7	56	147
CW724F	69.12	0.37	14.35	1.45	1.31	0.05	1.38	2.03	4.39	4.12	0.16	1.12	99.85	162	13	391	156
CW724G	70.63	0.37	14.47	1.31	1.34	0.05	1.16	2.17	3.79	4.06	0.17	0.73	100.25	146	12	421	157
Tin Fouga																	
CW714A	73.04	0.27	13.37	0.71	1.03	0.04	0.62	1.00	7.17	2.21	0.12	0.68	100.26	161	15	252	216
CW 97	74.77	0.01	13.31	0.12	0.97	0.04	0.04	0.63	4.38	4.43	0.03	0.57	99.30	81	9	108	144
CW151C	62.69	0.72	14.64	2.81	2.38	0.09	1.02	5.42	3.07	4.15	0.35	1.42	98.76	227	23	868	75
CW169D	70.04	0.28	14.08	1.04	0.81	0.06	0.62	1.70	4.41	4.52	0.10	1.08	98.74	183	16	343	179
CW227C	57.33	0.62	16.01	1.00	5.62	0.11	4.37	6.98	2.39	2.78	0.23	2.27	99.71	186	17	682	80
CW325B	54.33	0.66	15.34	1.33	7.25	0.14	5.47	9.75	0.59	2.53	0.21	1.91	99.51	177	15	709	12
CW333A	58.30	0.87	17.39	1.90	3.72	0.06	1.73	5.32	3.06	4.63	0.35	1.36	98.69	257	23	823	182

the geochemistry unit of the MRAC (J. Navez).

For the present geochemical study, three magmatic groups have been established: (1) *the volcanites* (2098 Ma), coming from the Birimian sequences, grades from basalts to rhyolites; (2) *the batholith* (2098–2073 Ma), groups the Massigui, Doubalakoro and Sirakoro granitic plutons containing magmatic intermediate or basic inclusions. No xenoliths have been included; (3) *the intermediate plutons* (2073 Ma), group the Sodioula and the Diélé plutons, mainly granodioritic but with some granitic facies and basic inclusions.

The three groups lie in the high-potassic calc-alkaline field of Peccerillo and Taylor (1976, Fig. 6a, SiO_2 versus K_2O). The intermediate plutons appear to be more potassic than the batholith in the range 63–68% SiO_2. The more acid varieties of the different groups can be relatively rich in K_2O (5–7%). No sodic or trondhjemitic trends are found in the studied area as described in the Mako Series in Sénégal (Débat et al., 1984) nor tholeiitic affinities (e.g. Fabre et al., 1987). Our granitoids and volcanics look more like the Daléma volcano-

plutonic complex from Sénégal (Bassot, 1987).

The SiO_2 versus agpaitic index (molecular Na+K/Al, Fig. 6b) diagram clearly shows the important increase of alkalies during differentiation for the three groups, the most acidic samples being close to or, for two of them, in the peralkaline field. In this figure has been reported the lower limit of the Iforas alkaline granites (agpaitic index=0.88, Liégeois and Black, 1987) where the end of our calc-alka-

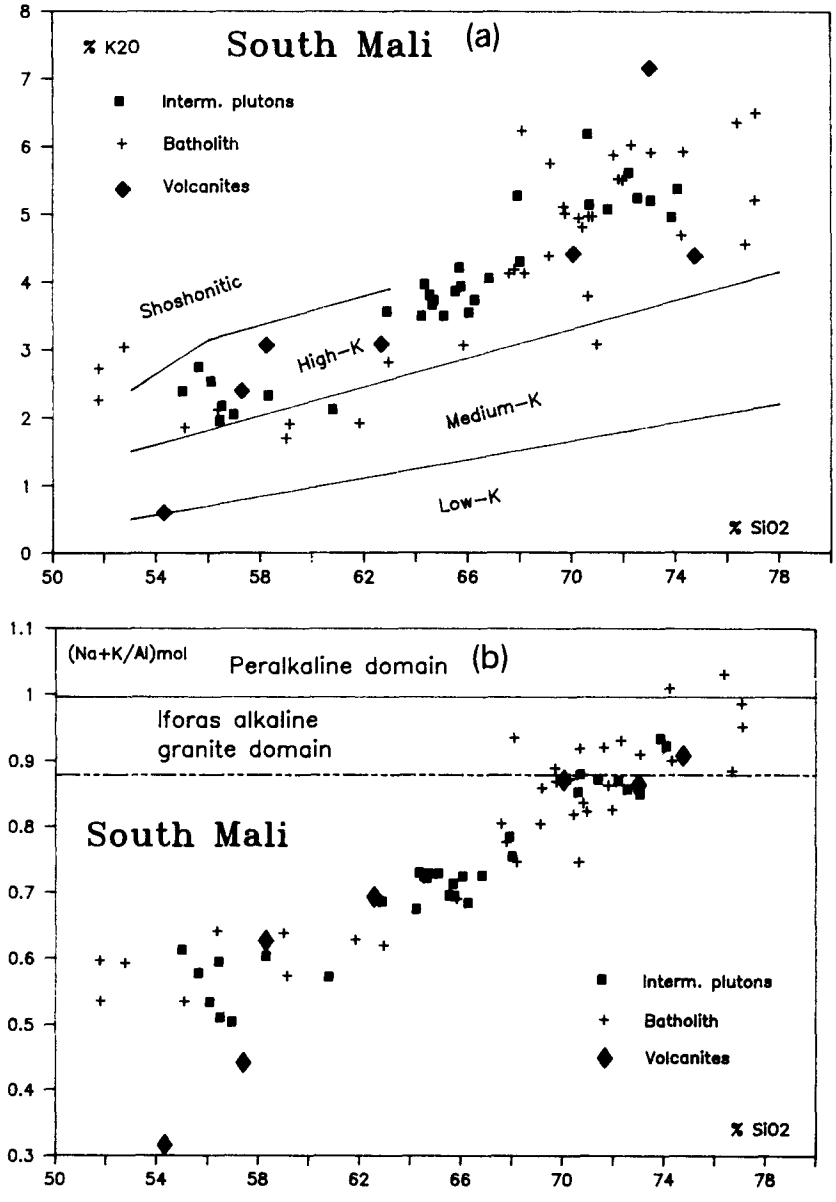

Fig. 6. (a) SiO_2 versus K_2O diagram (see text). (b) SiO_2 versus (Na+K)/Al (atomic proportion) diagram. The Iforas alkaline granite domain represents the area where are located the post-tectonic alkaline ring-complexes of the Adrar des Iforas (NE Mali; Liégeois and Black, 1987). This is an example showing that the more differentiated calc-alkaline granites of South Mali have a similar major elements geochemistry to that of classic alkaline granites. (c, overleaf) SiO_2 versus MgO diagram showing that plutons considered together in this study have sometimes distinctive features. A more detailed geochemical study would take into account this observation.

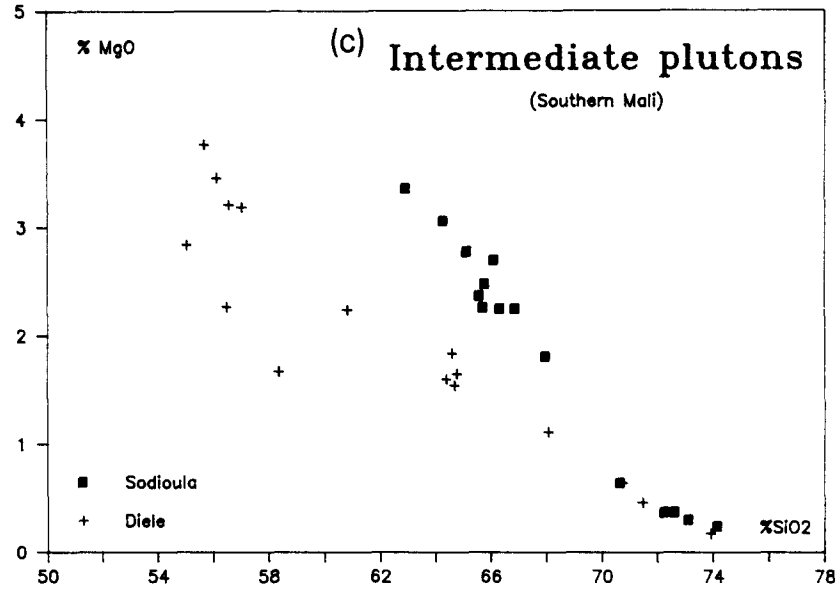

Fig. 6. Continued.

line trend lies. This alkaline affinity for the most differentiated samples is confirmed by the petrography of these rocks as they fall in the alkali granite domain of Streckeisen (1974), the felsic minerals being quartz and K-feldspar, with a very small amount of plagioclase. Moreover blueish amphibole is present. In fact, in the modal quartz–plagioclase–K-feldspar Streckeisen diagram, the studied magmatic suite shows a classical calc-alkaline trend beginning with diorites evolving to quartz-monzonites, granodiorites, monzo-granites and syeno-granites and even to alkali granites. In this case, alkali granites appear to be the ultimate product of a highly differentiated calc-alkaline series.

The defined calc-alkaline trend is in fact a composite trend as it is shown in Fig. 6c (SiO_2 versus MgO): the two intermediate plutons, Sodioula and Diélé, form two distinct trends. However, the aim of this paper is not to give a comprehensive geochemical study and as a first approach, one single, even composite, high-K calc-alkaline trend can be assumed.

The alkali granites of southern Mali are akin to the calc-alkaline suite. This is confirmed by the discrimination diagram of Pearce et al. (1985) SiO_2 versus log Y (Fig. 7a) where the most differentiated samples clearly fall in the volcanic arc–collision granites domain and far from the within-plate domain, the classical geodynamic environment of alkaline granites belonging to the alkaline suite. The three studied groups show similar trends in this diagram.

Although one must be very careful in the use of current discrimination diagrams based on Phanerozoic and Upper Proterozoic granites for evaluating geodynamic environments 2000 Ma ago, they do show constraining features. Some recent well-constrained studies on old terrains can favour plate tectonics models even in the Archaean (Davis et al., 1989).In the SiO_2 versus log Rb diagram (Pearce et al., 1985, Fig. 7b), the South Mali suite crosses the boundary between VAG (volcanic arc granites) and syn-COLG (syn-collision granites) around 68% SiO_2. Then if we consider only the granites stricto sensu, they lie only in the syn-COLG area but not far from the VAG field. Indeed, it is clear that the South Mali calc-alkaline suite does not correspond to a classical crustal leucogranite such as the Himalayan Manaslu granite (Le Fort, 1981; Vidal et al., 1982): the South Mali granites are linked to a

complete suite including an early dioritic stage, are not peraluminous and show in the field sharp contacts with the country rocks. If they are linked to a sort of collision, the latter has chances to look like a docking as in the Pan-African collision (600 Ma) in the Adrar des Iforas in Mali (Liégeois and Black, 1987; Liégeois et al., 1987). There, the collision granitoids define a high-K calc-alkaline suite with numerous subduction characteristics. More data are necessary to assess this hypothesis and there is no doubt that in such an intermediate

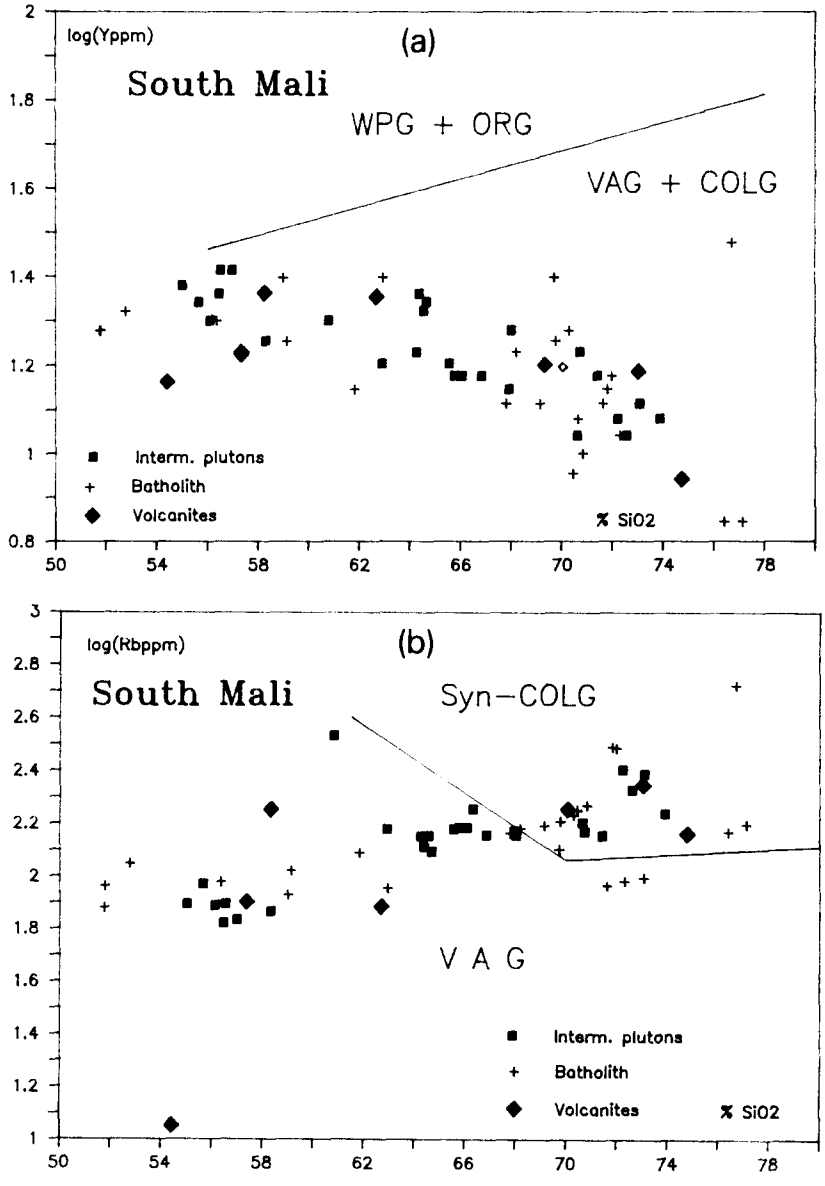

Fig. 7. (a) SiO_2 versus log Y, with the boundaries between WPG (within plate granite)–ORG (ocean ridge granite) and VAG (volcanic arc granite)–COLG (collision granite) (from Pearce et al., 1985). In contrast to major elements, trace elements show clearly the distinctive features of the studied differentiated calc-alkaline granites relative to the alkaline within-plate granites. (b) SiO_2 versus log Rb with the boundary separating the syn-COLG (syn-collision granite) and VAG (volcanic arc granite) (from Pearce et al., 1985). See text for details. (c, overleaf) Rb versus K_2O showing the high content of K_2O relatively to Rb of the South Mali granitoids.

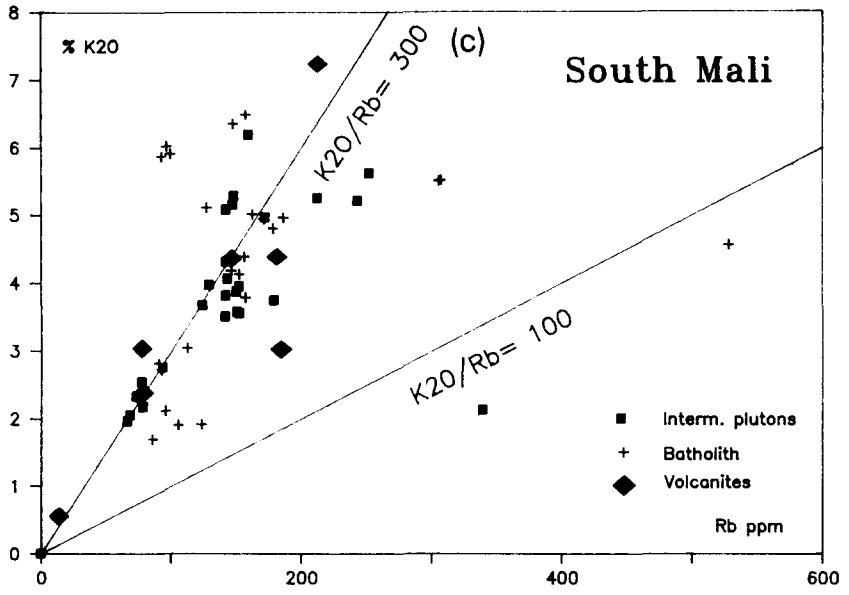

Fig. 7. Continued.

case, the discrimination diagrams are only a first step.

The phenomenon at the origin of the potassic enrichment of the South Mali suite has not induced a comparative enrichment in Rb, as shown in Fig. 7c (Rb versus K_2O): the mean K_2O/Rb ratio of the three groups is around 300 which is at the upper boundary of the main trend of Shaw (1968).

As a consequence, the mean Rb/Sr ratios of the different plutons are relatively low for high-K rocks (around 1), and the rehomogeneised SrIR 100 Ma after the intrusions are not much higher than the intrusive one.

The $^{87}Sr/^{86}Sr$ initial ratios (SrIR) of the different studied units are:

- Birimian volcanics: 0.7018 ± 0.0002 (2098 Ma);
- Granitic batholith: 0.7021 ± 0.0003 (2091 Ma);
- Sodioula granodiorite: 0.7015 ± 0.0005;
- Diélé granodiorite: 0.7014 ± 0.0005.

The values for Sodioula and Diélé have been calculated back to 2073 Ma (U–Pb on zircon age of Sodioula) assuming that the mean Rb/Sr ratio of each pluton has not changed during the isotopic rehomogeneisation linked to the D_3 deformation. The errors are given to take into account the uncertainty of these mean Rb–Sr ratios. In all cases, the magmatic initial ratios of Sodioula and Diélé must be lower than 0.7025 as it is the $^{87}Sr/^{86}Sr$ ratio given by the two isochrons around 1980 Ma for the two plutons. Even a little lower, which may be due to an open system during D_3, these two calculated SrIR are in the range of the two measured ones.

The SrIR of the volcanics are similar to those of the plutonites, both being relatively low, around 0.7020 or lower. As their chemistry and their age are in the same range, it is likely that they all come from the same evolving source. What could be this source? The more depleted MORB would have at 2100 Ma a $^{87}Sr/^{86}Sr$ ratio of 0.7006 [with present-time values of 0.702 ($^{87}Sr/^{86}Sr$) and 0.045 ($^{87}Rb/^{86}Sr$); Faure, 1977]; a mean for modern island arcs would have a value of 0.7017 (with present 0.704 and 0.075; Faure, 1977). The Pan-African Tilemsi island arc (Liégeois, 1988; Caby et al., 1986) gives, calculated back to 2100 Ma, a similar value of 0.7015 (with 600 Ma values respectively of 0.703 and 0.069). The depleted mantle at 2100 Ma under the Canadian shield

is also round 0.7015–0.7016 (Bell and Blenkinsop, 1987).

A subduction source, i.e., a mixture of peridotitic mantle and subducted oceanic crust materials, would have then a mean $^{87}Sr/^{86}Sr$ ratio 2100 Ma ago around 0.7015–0.7017. This ratio is similar to the Diélé and Sodioula calculated ratios, compatible, within error limits, with the SrIR of the volcanics and a little lower than that of the batholith. A high-pressure granulitic lower crust is, for the $^{87}Sr/^{86}Sr$ ratios, another possible source at it can be depleted in Rb (Sighinolfi, 1971). However, it is very unlikely that such a refractory material could produce such an important volume of magmas as present in the Birimian. On the contrary, a participation of a Rb-depleted lower crust as a contaminant in the Birimian and Eburnian magma genesis is possible and would explain, if this phenomenon is important, the high K/Rb ratios of these magmas. Nd or Pb isotopes are necessary to assess this hypothesis.

The field work has shown the existence of volcano-sedimentary inclusions in the plutonites. However, the amount of the contamination of the batholith by this material cannot be estimated as both SrIR and geochemistry of contaminant and contaminated material are very similar.

In conclusion, a same source for the Birimian volcanites and for the Eburnian plutonites can be proposed as both magmatisms have similar geochemistry, $^{87}Sr/^{86}Sr$ initial ratios, and occurred in a small period of time (2100–2070 Ma). In the studied area, the Birimian volcanites can be included in the Eburnian magmatism, which is then entirely calc-alkaline as in the Daléma complex (Bassot, 1987).

This source has produced a high-K calc-alkaline suite from a dioritic stage to monzogranites but also to syeno-granites and alkali granites (Streckeisen sense). Let us insist that the latter have clearly calc-alkaline affinities, distinct from classical within-plate alkaline granites.

This suite proceeds from a subduction-type or docking-type mantle source with virtually no old crustal component except if it is strongly Rb-depleted. The interaction batholith–volcano-sedimentary series seen in the field cannot be quantified as they have very similar geochemical and Sr isotopic characteristics.

Our Massigui area has similar and distinct features with greenstone belts. Firstly, a comparison is only possible with upper parts of these Archaean belts as both komatiites and tholeiitic volcanics are absent, which are typical of the lower parts (e.g. Anhaeusser, 1981; Windley, 1984). Similarities are the association of volcanics and immature sediments affected by greenschist facies metamorphism which can reach the amphibolite facies on the edges of the belts, near granitic batholiths, the importance of horizontal tangential tectonics and shear tectonics (e.g. Stowe, 1974; Coward et al., 1976), gold mineralization in the volcanics and Sn, Li, Be in granitic and pegmatitic bodies. Dissimilarities are the absence of old gneisses, the high-K calc-alkaline chemistry of pre- to syn-tectonic magmatism (low-K in greenstone belts) and the fact, if our convictions are confirmed, that, with time, the volcano-sedimentary assemblage becomes more volcanic, which is the opposite of classical greenstones (Lowe, 1982). A complete comparison with greenstone belts is not possible without taking into account other areas of the northwest Man shield even only in Mali, such as southern Mali areas studied by the UNDP mission (Diallo and Kusnir, 1985) were basaltic pillow lavas and ultramafic bodies are known to occur, or as western Mali where tholeiitic volcanics and shallow-water sediments including carbonates are present (Klöckner mission, pers. commun.).

General conclusions

The combination of extensive field, Rb–Sr on whole-rock and U–Pb on zircon geochronology and geochemistry studies on the Massigui area allow us to propose some regional con-

TABLE 4

Evolution of the Eburnian orogeny in South Mali (this paper).

Ma	LITHOLOGY	TECTONICS	METAMORPHISM
1982 +/−30	Pegmatites?	D3: reactivation of the Banifin corridor.	Local (Banifin) retrograde metam. (greenschist)
2074 +/−7	Calc–alkaline interm. plutons (Banifin)	D2: Regional shear tectonics, steeply dipping fold axis max. intensity in the Banifin zone	Regional highgrade greenschist + local (Banifin) low–grade amphibolite facies
2091 +/−33	Calc–alkaline granitic batholiths (West)		
2098 +/−5	Preponderant (Centre) calc–alkaline volcanites	D1: regional tangential tectonics	?
	Preponderant sediments pelitic (East) clayey sand (Centre)		

straints on the Eburnian orogeny sensu stricto north of the Man shield (the older so-called Burkinian orogeny is not present) (Table 4).

– In southern Mali, the Eburnian orogeny begins with deposition of immature clastic sediments (basement unknown) progressively invaded by volcanics (2098 ± 5 Ma) mainly of andesitic composition, the whole process likely being a unique phenomenon occurring in a relatively short period of time. No trace of an old basement has been found.

– Subsequent plutonism with similar geochemical characteristics as the volcanics, is somehow linked to the regional deformation as it is early- or syn-tectonic (2091 ± 33 Ma and 2073 ± 7 Ma) and as the deformation is much stronger along the huge granitic batholith (Banifin shear belt).

– This shear belt has defined a zone of weakness one hundred million years later (1982 ± 30 Ma), where tectonic reactivation and Sr isotopes rehomogeneisation occurred.

– The regional deformation appears to have comprised a first phase with a likely main tangential regime and has evolved in a second phase characterized by a main shear component.

– Sr initial ratios indicate a largely proponderant mantle source for both volcanics and plutonites, in agreement with the lack of old basement, and geochemistry points to a high-K calc-alkaline magmatism with subduction or docking characteristics for both.

This implies that the Eburnian orogeny in southern Mali was short-lived (~ 30 Ma, between 2100 Ma and 2070 Ma). However, taking into account the width of the Birimian domain of the West African craton, a diachronism between several dockings of Massigui type which may have occurred, must be envisaged. The term "Eburnian orogen" comprises as well the Birimian volcanics as the granitic plutonism which must be fondamentally linked.

A major reactivation occurred 100 Ma later, around 1980 Ma ago, apparently without associated magmatism, which reset completely the Rb–Sr isotopic system in the Banifin corridor. If this is a regional phenomenon, as our

current studies in the Malian part of Kayes and Kenieba inliers seem to attest, it would explain the second peak of ages of Tempier et al. (1987) and brings caution on the old chronology based only on Rb–Sr systematics.

Acknowledgements

This paper is based on a comprehensive field survey which has resulted from a cooperation between the Malian and the Belgian governments through the Direction Nationale de la Géologie et des Mines (DNGM, Mali) and the Agence Générale de la Coopération au Développement (AGCD, Belgium) with the technical assistance of the Department of Geology of the Musée Royal de l'Afrique Centrale (MRAC, Belgium) and of BUGECO (Belgium).

We thank R. Black for discussions and for his help in English, K. Theunissen for discussions on deformation problems. J.M. Bertrand and an anonymous reviewer for constructive reviews of this paper.

References

Agyei, E.K., Van Landewijk, J.E.J.M., Armstrong, R.L., Harakal, J.E. and Scott, K.L., 1987. Rb–Sr and K–Ar geochronometry of southeastern Ghana. J. Afr. Earth Sci., 6: 153–161.

Anhaeusser, C.R., 1981. Geotectonic evolution of the Archaean successions in the Barberton Mountain Land, South Africa. In: A. Kröner (Editor), Precambrian Plate Tectonics. Amsterdam, Elsevier, pp. 137–160.

Barinkov, I.P. and Novikov, A.G., 1966. Rapport sur le levé aéromagnétique dans la partie sud du Mali. Arch. Dir. Gén. Géol. Mines, Bamako, Mali, Sonarem.

Barning, K., 1987. The Birimian system of West Africa: case studies in Ghana and Ivory Coast. XIV Coll. Afr. Geol., Berlin.

Bassot, J.P., 1987. Le complexe volcano-plutonique calco-alcalin de la rivière Daléma (Est Sénégal): discussion de sa signification géodynamique dans le cadre de l'orogénie éburnéenne (Protérozoïque inférieur). J. Afr. Earth Sci., 6: 505–519.

Bassot, J.P. and Caen-Vachette, M., 1984. Données géochronologiques et géochimiques nouvelles sur les granitoïdes de l'Est Sénégal: implications sur l'histoire géologique du Birrimien de cette région. In: J. Klerkx and J. Michot (Editors), Géologie Africaine. Mus. Roy. Afr. Centr., Tervuren, pp. 191–209.

Bassot, J.P., Meloux, J. and Traore, H., 1981. Notice explicative de la carte géologique à 1 : 1,500,000 de la république du Mali. Arch. Dir. Gén. Géol. Mines, Bamako, Mali.

Bell, K. and Blenkinsop, J., 1987. Archean depleted mantle: evidence from Nd and Sr initial isotopic ratios of carbonatites. Geochim. Cosmochim. Acta, 51: 291–298.

Bertrand, J.M., Dia, A., Dioh, E. and Bassot, J.M., 1989. Réflexions sur la structure interne du craton Ouest-Africain au Sénégal oriental et confins guinéo-maliens. C.R. Acad. Sci. Paris, 309, Sér. II: 751–756.

Bessoles, B., 1977. Géologie de l'Afrique. Le craton ouest-africain. Mémoires BRGM, Paris, 88: 402 pp.

Black, L.P., 1987. Recent Pb loss in zircon: a natural or laboratory-induced phenomenon? Chem. Geol., 65: 25–33.

Black, R., 1980. Precambrian of West Africa. Episodes, 4: 3–8.

Buchstein, M., Cisse, S. and Sikosso, I., 1974. Recherches géologiques et minières dans la région de Bougouni–Sikasso–Ganfolila. Rapp. BRGM no. 74 DAK 001 bis, Dir. Nat. Géol. Mines, Bamako, Mali (unpublished).

Caby, R., Liégeois, J.P., Dostal, C., Dupuy, C. and Andreopoulos-Renaud, U., 1986. The Tilemsi magmatic arc and the Pan-African suture zone in northern Mali. Int. Field Conf. on Proterozoic Geology and Geochemistry. Colorado, USA, p. 88.

Cliff, R.A., 1985. Isotopic dating in metamorphic belts. J. Geol. Soc. London, 142: 97–110.

Coward, M.P., Lintern, B.S. and Wright, L.I., 1976. The pre-cleavage deformation of the sediments and gneisses of the northern part of the Limpopo belt. In: B.F. Windley (Editor), The Early History of the Earth. Wiley-Interscience, London, pp. 323–330.

Davis, D.W., Poulsen, K.H. and Kamo, S.L., 1989. New insight into Archean crustal development from geochronology in the Rainy Lake area, Superior Province, Canada. J. Petrol., 7: 379–398.

Débat, P., Diallo, D.P., Ngom, P.M., Rollet, M. and Seyler, M., 1984. La série de Mako dans ses parties centrale et méridionale (Sénégal Oriental, Afrique de l'Ouest). Précision sur l'évolution de la série volcano-sédimentaire et données géochimiques préliminaires sur les formations magmatiques post-tectoniques. J. Afr. Earth Sci., 2: 71–79.

Diallo, M., and Kusnir, I., 1985. Résultats des travaux de prospection de la région aurifère de la Bagoé (Projet "Or Bagoé"). Arch. Dir. Nat. Géol. Mines, Bamako, Mali.

Dott, R.H., 1964. Wacke, graywacke and matrix – what approach to immature sandstone classification? J. Sediment. Petrol., 34: 525–532.

Fabre, R., Matheis, G. and Utke, A.W., 1987. Caractéris-

ation géochimique du magmatisme birrimien dans le centre de la Côte d'Ivoire (Afrique de l'Ouest): ses implications géodynamiques. In: G. Matheis and J. Schandelmeier (Editors), Current Research in African Earth Sciences. Balkema, Rotterdam, pp. 21–24.

Faure, G., Ed. 1977. Principles of Isotope Geology, Wiley, New York, 464 pp.

Feybesse, J.L., Milési, J.P. Johan, V., Dommanget, A., Calvez, J.Y., Boher, M. and Abouchami, W., 1989. La limite Archéen/Protérozoïque inférieur d'Afrique de l'Ouest: une zone de chevauchement majeure antérieure à l'accident de Sassandra; L'exemple des régions d'Odiénné et de Touba (Côte-d'Ivoire). C.R. Acad. Sci. Paris, 309, sér. II: 1847–1853.

Hurley, P.M., Almeida, F.F.M., Melcher, G.C., Cordani, U.G., Rand, J.R., Kawashita, K., Vandoros, P., Pinson, W.H. and Fairbairn, H.W., 1967. Test of continental drift by comparison of radiometric data. Science, 157: 495–500.

Krogh, T.R., 1973. A low contamination method for hydrothermal decomposition of zircon and extraction of U and Pb for isotopic age determination. Geochim. Cosmochim. Acta, 37: 485–494.

Lancelot, J.R., 1975. Les systèmes U–Pb chronomètres et traceurs de l'évolution des roches terrestres. Thèse Université Paris VII, 280 pp.

Ledent, D., Delhal, J. and Trinquard, R., 1969. Ages par la méthode Pb/U de granites "éburnéens" de Haute-Volta. Comparaison avec des résultats obtenus par la méthode Sr/Rb sur roches totales et sur biotites. Ann. Soc. Géol. Belg., 92: 258–292.

Ledru, P., Milési, J.P., Feybesse, J.L., Dommanget, A., Johan, V., Diallo, M. and Vinchon, C., 1989. Tectonique transcurrente et évolution polycyclique dans le Birrimien, Protérozoïque inférieur, du Sénégal–Mali (Afrique de l'Ouest). C.R. Acad. Sci. Paris, 308, sér. II: 117–122.

Le Fort, P., 1981. Manaslu leucogranite: a collision signature of the Himalaya. A model for its genesis and emplacement. J. Geophys. Res., 16: 10545–10568.

Legrand, J.M., 1971. Précisions sur l'évolution du cycle birrimien obtenues par de nouvelles mesures d'âges par la méthode U/Pb sur des zircons de granites éburnéens de Haute Volta. Ann. Soc. Géol. Belg., 94: 237–248.

Lemoine, S., Tempier, P., Bassot, J.P., Caen-Vachette, M. and Vialette, Y., 1986. Some geochemical and geotectonic features of the two lower Proteozoic orogenies in West Africa. In: K.C. Condie (Editor), Proterozoic Geology and Geochemistry. IGCP 215 & IGCP 217, Central Colorado, p. 107.

Lesquer, A., Beltrao, H.F. and De Abreu, F.A.M., 1984. Proterozoic links between northeastern Brazil and West Africa: a plate tectonic model based on gravity data. Tectonophysics, 100: 9–26.

Liégeois, J.P., 1988. Le batholite composite de l'Adrar des Iforas (Mali). Acad. R. Sci. Outre-Mer Classe Sci. Nat. Méd., Mém. in 8°, nouvelle série, no. 22. Bruxelles, 231 pp.

Liégeois, J.P. and Black, R., 1987. Alkaline magmatism subsequent to collision in the Pan-African belt of the Adrar des Iforas (Mali). In: J.G. Fitton and B.J.G. Upton (Editors), Alkaline Igneous Rocks. Geol. Soc. Spec. Publ. 30, London, pp. 381–401.

Liégeois, J.P., Bertrand, J.M. and Black, R., 1987. The subduction- and collision-related Pan-African composite batholith of the Adrar des Iforas (Mali): a review. Geol. J., 22: 185–211.

Lowe, D.R., 1982. Comparative sedimentology of the principal volcanic sequences of Archean greenstone belts in South Africa, W. Australia, and Canada: implications for crustal evolution. Precambrian Res., 17: 1–29.

Ludwig, K.R., 1980. Calculation of uncertainties of U–Pb isotope date. Earth Planet. Sci. Lett., 46: 212–220.

Milesi, J.P., Dommanget, J.L., Feybesse, J.L., Ledru, P., Diallo, M. and Keita, F., 1987. Quelques questions sur les séries du Protérozoïque inférieur de l'Afrique de l'Ouest. In: G. Matheis and H. Schandelmeier (Editors), Current Research in African Earth Sciences, Berlin, pp. 7–8.

Ndiaye, P.M., Robineau, B. and Moreau, C., 1989. Déformation et métamorphisme des formations birrimiennes en relation avec la mise en place du granite éburnéen de Saraya (Sénégal oriental). Bull. Soc. Géol. France, 8(V): 619–625.

Paterson, S.R. and Tobisch, O.T., 1988. Using pluton ages to date regional deformations: problems with commonly used criteria. Geology, 16: 1108–1111.

Pearce, J.A., Harris, N.B.W. and Tindle, A.C., 1985. Trace element discrimination diagrams for the tectonic interpretation of granitic rocks. Contr. Mineral. Petrol., 69: 33–47.

Peccerillo, A. and Taylor, S.R., 1976. Geochemistry of Eocene calc-alkaline volcanic rocks from the Kastomu area, northern Turkey. Contr. Mineral. Petrol., 58: 63–81.

Shaw, D.M., 1968. A review of K–Rb fractionation trends by covariance analysis. Geochim. Cosmochim. Acta, 32: 573–601.

Sighinolfi, G.P., 1971. Investigations into deep crustal levels: fractionating effects and geochemical trends related to high-grade metamorphism. Geochim. Cosmochim. Acta, 35: 1005–1021.

Spindler, J.P., 1952. Rapport géologique. Fin de campagne 1950–1951 (feuille Bougouni Est). Arch. Dir. Mines A.O.F., Dakar, 124 pp. (unpublished).

Steiger, R.H. and Jäger, E., 1977. Subcommission on geochronology: convention on the use of decay constants in geo- and cosmochronology. Earth Planet. Sci. Lett., 36: 359–362.

Stowe, C.W., 1974. Alpine-type structure in the Rhode-

sian basement complex at Selukwe. J. Geol. Soc. London, 130: 411–426.
Streckeisen, A.L., 1974. Classification and nomenclature of plutonic rocks. Geol. Rundsch., 63: 773–786.
Tempier, P., Bassot, J.P., Caen-Vachette, M., Kone, M., Lemoine, S., Toure, S., Vialette, Y. and Wenmenga, U., 1987. Les massifs intrusifs et annnulaires du Protérozoïque inférieur en Afrique de l'Ouest. Leur signification dans l'évolution du Protérozoïque inférieur de cette région. XIV Coll. Afr. Geol., Berlin, p. 58.
Toure, S., Caen-Vachette, M. and Tempier, P., 1987. Nouvelles données pétrographiques, géochimiques et géochronologiques du massif "granitique" de Bondoukou (Côte d'Ivoire) mise en évidence d'un âge burkinien, par isochrone Rb/Sr sur roches totales. J. Afr. Earth Sci., 6: 269–274.
Vidal, M., 1987. Les déformations éburnéennes de l'Unité birrimienne de la Comoé (Côte d'Ivoire). J. Afr. Earth Sci., 6: 141–152.
Vidal, M. and Alric, G., 1987. Une tectonique de coulissement et un volcanisme tholéiitique: spécificités du cycle éburnéen de Haute-Comoé (Côte d'Ivoire). In: G. Matheis and J. Schandelmeier (Editors), Current Research in African Earth Sciences. Balkema, Rotterdam, pp. 25–28.
Vidal, P., Cocherie, A. and Le Fort, P., 1982. Geochemical investigations on the origin of the Manaslu leucogranite (Himalaya, Nepal). Geochim. Cosmochim. Acta, 46: 2279–2292.
Williamson, J.H., 1968. Least squares fitting of a straight line. Can. J. Phys., 46: 1845–1847.
Windley, B.F., 1984. The Evolving Continents. Wiley, New York, 399 pp.